Review Article

Application of ionic liquids in single-molecule junctions: Recent advances and prospects

Li Zhou [a,1], Miao Zhang [a,1], Yani Huo [a], Liping Bai [a], Suhang He [a], Jinying Wang [a,b,*], Chuancheng Jia [a,*], Xuefeng Guo [a,c,*]

[a] *Center of Single-Molecule Sciences, Institute of Modern Optics, Frontiers Science Center for New Organic Matter, College of Electronic Information and Optical Engineering, Nankai University, 38 Tongyan Road, Jinnan District, Tianjin, 300350, China*
[b] *Network for Computational Nanotechnology, Purdue University, West Lafayette, IN, 47907, USA*
[c] *Beijing National Laboratory for Molecular Sciences, National Biomedical Imaging Center, College of Chemistry and Molecular Engineering, Peking University, 292 Chengfu Road, Haidian District, Beijing, 100871, China*

Abstract

Single-molecule junctions, integrating individual molecules as active components between electrodes, serve as fundamental building blocks for advanced electronic and sensing technologies. The application of ionic liquids in single-molecule junctions represents a cutting-edge and rapidly evolving field of research at the intersection of nanoscience, materials chemistry, and electronics. This review explores recent advances where ionic liquids function as electrolytes, dielectric layers, and structural elements within single-molecule junctions, reshaping charge transport, redox reactions, and molecular behaviors in these nanoscale systems. We comprehensively dissect fundamental concepts, techniques, and modulation mechanisms, elucidating the roles of ionic liquids as gates, electrochemical controllers, and interface components in single-molecule junctions. Encompassing applications from functional device construction to unraveling intricate chemical reactions, this review maps the diverse applications of ionic liquids in single-molecule junctions. Moreover, we propose critical future research topics in this field, including catalysis involving ionic liquids at the single-molecule level, functionalizing single-molecule devices using ionic liquids, and probing the structure and interactions of ionic liquids. These endeavors aim to drive technological breakthroughs in nanotechnology, energy, and quantum research.

1. Introduction

Single-molecule junctions are nanoscale devices that incorporate individual molecules as active components, serving as fundamental building blocks for advanced electronic and sensing technologies [1–4]. Single-molecule junctions not only meet the increasing technical requirements of device miniaturization and functionalization [5], but are also powerful tools for uncovering novel mechanisms at the molecular scale [6]. These two aspects of research complement one another synergistically. On one hand, we can exert precise control over the electronic behavior within single-molecule junctions through methods such as molecular modification [7–10], gate voltage manipulation [11−15], and interface engineering [16–20]. This allows us to delve into novel physical and chemical processes and mechanisms. On

* Corresponding authors. Center of Single-Molecule Sciences, Institute of Modern Optics, Frontiers Science Center for New Organic Matter, College of Electronic Information and Optical Engineering, Nankai University, 38 Tongyan Road, Jinnan District, Tianjin, 300350, China.
E-mail addresses: wang4205@purdue.edu (J. Wang), jiacc@nankai.edu.cn (C. Jia), guoxf@pku.edu.cn (X. Guo).
[1] These authors contributed equally to this work.

the other hand, we can harness these newfound insights to inform and enhance the design and optimization of molecular devices [6,21]. Ultimately, this iterative process leads to the development and application of high-performance functionalized devices.

Ionic liquids, which are salts composed of cations and anions in liquid form at or near room temperature, have emerged as a fascinating and versatile tool with immense potential. They have a lot of unique properties, such as high charge density [22,23], wide electrochemical window [24], low vapor pressure [25], tunable polarity [26], etc. The utilization of ionic liquids in single-molecule junctions offers a range of unique advantages. These specialized liquids can serve as electrolytes, dielectric layers, and even structural components within these nanoscale devices [13,27]. Their ability to efficiently transport ions, wide electrochemical stability window, tunable properties, and reduced volatility make them exceptionally well-suited for regulating charge transport, redox reactions, and the overall behavior of single-molecules in these junctions [28–30]. For example, 1-butyl-3-methyl-imidazolium hexafluorophosphate ($[BMI]^+[PF_6]^-$) can serve as a conducive medium in scanning tunneling microscope measurements by effectively reducing the resistance encountered during the data acquisition process, owing to its high intrinsic ionic conductivity [31]. This intrinsic characteristic of $[BMI]^+[PF_6]^-$ greatly facilitates the acquisition of important information about the charge transfer process, allowing researchers to glean valuable insights into the underlying mechanisms [31]. The application of ionic liquids in single-molecule junctions represents a cutting-edge and rapidly evolving field of research at the intersection of nanoscience, materials chemistry, and electronics. The deep understanding of the relevant mechanisms and applications are not only advancing our fundamental understanding of molecular-scale electronics, but also paving the way for the development of novel, high-performance nanoscale devices.

In this review, we summarize the recent advances in application of ionic liquid in single-molecule junctions. We start with the fundamentals concepts and techniques including the preparation methods of single-molecule junctions and the construction of junctions in ionic liquids. Then, the modulation mechanisms of ionic liquids in single-molecule junctions are emphasized, including how ionic liquids serve as gate, electrochemical controller, and molecule-electrode interface controls. The applications of ionic liquids in single-molecule junctions including the construction of functional devices and the exploration of chemical reaction mechanism are overviewed. Finally, we propose the future research directions, encouraging the exploration of scientific problems in the field of physics and chemistry from the perspective of molecules and even atoms.

2. Construction of single-molecule junctions within ionic liquids

In recent years, significant strides have been made in the utilization of ionic liquids into single-molecule junctions. The construction of single-molecule junctions within ionic liquids necessitates meeting three essential criteria: (1) a nanogap between electrodes matching the molecular size, (2) a reliable and efficient connection between the molecule and the electrodes, and (3) efficient introduction of ionic liquids. In this chapter, we introduce the typical construction techniques of single-molecule junctions, analyze the selection factors of ionic liquids, and summarize the design and construction strategies of single-molecule junctions within ionic liquids.

2.1. Construction methods of single-molecule junctions

Single-molecule junctions are composed of nanogap electrodes, the contact interface, and the molecular backbone [21]. The preparation techniques of these junctions can be classified into two primary categories based on the type of nanogap electrode: "static" and "dynamic" molecular junctions [32]. Static molecular junctions are constructed using micro-nano fabrication technologies, where the size of the nanogap electrodes remains fixed [14,33–35]. They offer a relatively stable molecular electrode connection which helps to stabilize the drive performance [35]. In contrast, dynamic molecular junctions are formed by controlling the opening and closing of a metal electrode pair [32]. This approach enables the repeated constructions of single-molecule junctions, facilitating the generation of a substantial volume of conductance data for statistical analysis [36–39].

2.1.1. Static molecular junctions

Static molecular junctions are characterized by the fixed nanogap and molecular positions. Currently, two primary methods are employed to create static molecular junctions. One approach involves the direct assembly of molecules, followed by the placement of a top electrode [40,41]. The alternative method firstly constructs the electrode pairs before proceeding with molecular assembly, such as electromigration [33,42] and etching processes [43,44]. In this section, we focus on the latter method. Fig. 1a and b show the schematic for constructing static single-molecular junctions.

Electromigration is a phenomenon where atoms migrate under the influence of an external electric field. By applying a bias voltage to metal nanowires, they can be induced to fracture, creating nanogap electrodes [14,45]. However, excessive current density can lead to the formation of large nanogaps and metal islands within them, resulting in unpredictable electrode separation and interfering with the intrinsic molecular signal [34]. To precisely control the nanogap size using the electromigration technology, significant research efforts have been undertaken. One effective approach involves regulating the migration current, exemplified by a feedback-controlled electromigration technology [46]. This technique monitors changes in resistance during the incremental application of voltage ramps [46]. As the electromigration progresses, the metal electrode's resistance changes. When the conductance reaches a predefined threshold percentage of the initial value, the voltage is incrementally reduced to prevent nanowire breakage. This process is repeated until a nanogap of less than 1 nm is achieved. Similar to the electromigration of
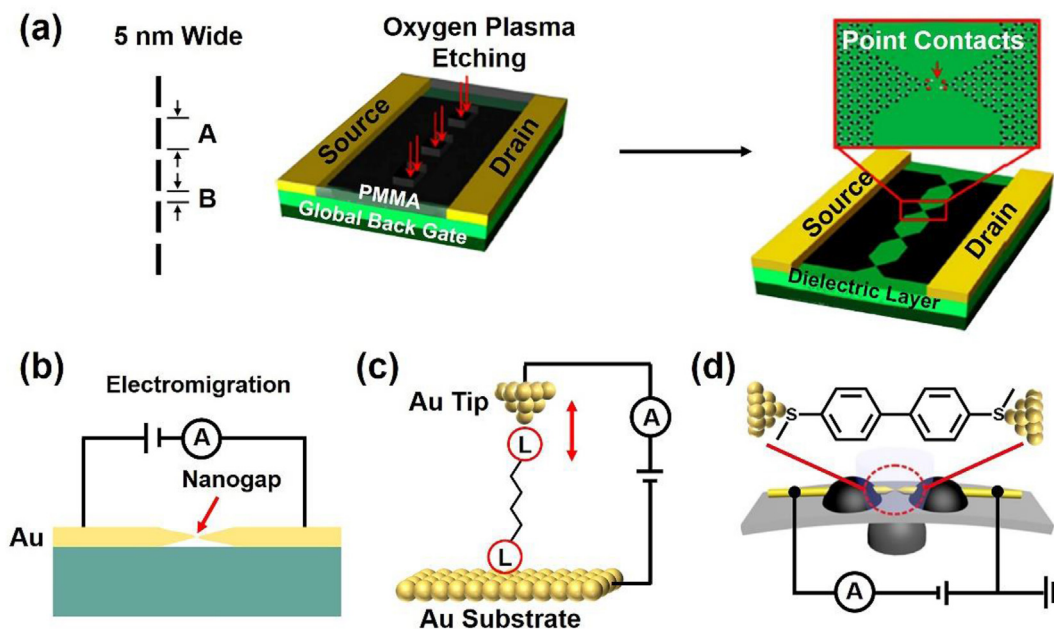
Fig. 1. Construction of static and dynamic molecular junctions. (a) Static single-molecular junctions with graphene point contacts through an etching processing technology. (reprinted with permission from Ref. [44] Copyright 2012 Wiley-VCH Verlag GmbH & Co. KGaA, Weinheim). (b) Static single-molecular junctions constructed by electromigration. (c) Dynamic molecular junctions constructed by scanning tunneling microscope break junctions (reprinted with permission from Ref. [54] Copyright 2007 American Chemical Society). (d) Mechanically controlled break junction technologies (reprinted with permission from Ref. [57] Copyright 2019 Wiley-VCH Verlag GmbH & Co. KGaA, Weinheim).

metal electrodes, applying high-density current to single-walled carbon nanotubes (SWCNT) or graphene can also lead to material breakdown [47,48]. Consequently, it is feasible to fabricate carbon-based nanogap electrodes using electromigration.

Another technique employed for creating static molecular junctions involves etching processing, particularly suited for constructing carbon-based nanogap electrodes [43,44]. For instance, this method has successfully enabled the formation of graphene point contact arrays on a single layer of graphene [44]. The process begins by firstly creating an array window pattern with equally spaced, 5 nm wide holes on PMMA-coated graphene through photolithography. Subsequently, precise etching of the exposed graphene is achieved using oxygen plasma etching, resulting in carboxyl-modified graphene point contact electrodes. Leveraging the amide condensation reaction, molecules featuring amino groups as anchor groups can be covalently bonded to these electrodes, ultimately forming stable single-molecule junctions (Fig. 1a). Compared to metal electrodes, carbon-based electrodes exhibit superior chemical stability. The connection of molecules to carbon-based electrodes via covalent bonds mitigates the issue of weak coordination bonds that are prone to breakage in metal electrode systems [44].

2.1.2. Dynamic molecular junctions

Dynamic molecular junctions are characterized by their dynamic alterations in the distance between electrode pairs. This dynamic feature enables the creation and disruption of molecular junctions through the repetitive approach and withdrawal of electrode pairs. Currently, three prevalent mechanical break junction techniques are employed to fabricate dynamic molecular junctions, including the atomic force microscopy break junction (AFM-BJ) [49], scanning tunneling microscope break junction (STM-BJ) [38,50,51], and the mechanically controlled break junction (MCBJ) [52,53]. Both AFM-BJ and STM-BJ are methods used to fabricate single-molecule devices employing scanning probe microscopes. The key distinction lies in the feedback mechanism: the AFM-BJ relies on the interaction force between the tip and the base, while the STM-BJ relies on tunnel current [6]. Therefore, the AFM-BJ can additionally study the force-related properties of molecules.

In the STM-BJ technology, precise control of the STM tip is achieved through a piezoelectric actuator, enabling it to approach or retreat from the substrate containing the target molecule and thereby dynamically forming a nanogap [6]. In detail, the molecules anchor to the electrode through their anchoring groups firstly. As the STM tip gradually moves away, only one molecule remains connected between the electrode pairs, resulting in the formation of a single-molecule junction (Fig. 1c) [54]. When the distance between the electrode pairs exceeds the molecular length, the single-molecule junction breaks. Simultaneously, the current data from the molecule is recorded in real time while the tip is in motion. By repeating this process, a substantial amount of conductance data is collected, subsequently consolidated into conductance histograms for comprehensive statistical analysis.

Another effective method to construct single-molecule junctions is the MCBJ technique. In this approach, a mechanical force is initially applied to the actuator via a stepper motor, causing the flexible substrate to bend [6,55]. This action subsequently subjects the nanowires on the flexible

substrate to lateral stress at the notch, leading to their breakage and the formation of a nanogap [6,56]. Similar to the process of creating single-molecule junctions with STM-BJ, the target molecule featuring an anchoring group bonds to the metal point electrode pairs, resulting in the creation of a single-molecule junction (Fig. 1d) [57]. Subsequently, as the pusher continues to move upward, the single-molecule junction breaks. When the tunneling current gradually decreases to a preset value, the push rod retracts, ultimately closing the electrode pair. The iterative up-and-down movements of the pusher continually generate nanogaps, thereby capturing target molecules and forming a multitude of molecular junctions.

In contrast to static molecular junctions, dynamic molecular construction techniques (such as STMBJ and MCBJ technologies) offer efficient and precise control over the nanoelectrode gap distance by utilizing tunneling current as a feedback signal [50,55]. Furthermore, these dynamic approaches are advantageous for acquiring statistical data regarding the electric transport properties of single molecules, thus enhancing the repeatability and reliability of research in this field [51,58].

2.2. Integration of ionic liquids in single-molecule junctions

Ionic liquids play a critical role in molecular electronics due to their diverse properties. Constructing high-performance single-molecule functional devices requires careful selection of appropriate ionic liquids. This selection process relies on a comprehensive understanding of the intrinsic physical properties of ionic liquids, as well as a deep understanding of their mechanisms of action within single-molecule devices. In this section, we summarize various types of ionic liquids commonly employed in single-molecule research. We discuss the unique properties of these ionic liquids and provide insights into the selection criteria essential for enhancing the device performance. Then, we elucidate the formation and characterization of the electric double layer (EDL) in ionic liquids, which is fundamental for understanding the role of ionic liquids within single-molecule junctions. Lastly, we
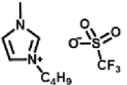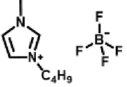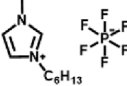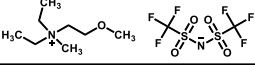
introduce the prototypical single-molecule junctions within ionic liquids, illustrating practical applications and optimizations of such devices leveraging the unique properties of ionic liquids.

2.2.1. Typical ionic liquids in single-molecule junctions

Ionic liquids, with their exceptional attributes including high ionic conductivity, a wide electrochemical window, high dielectric constants, low volatility and toxicity, find versatile applications as electrolytes, dielectric layers, and even structural constituents in various devices [24–26,59]. Currently, the predominant types employed in single-molecule junctions are quaternary ammonium and imidazole-based ionic liquids (Table 1) [60–68]. A profound comprehension of how to select proper ionic liquids within single-molecule junctions not only aids in developing high-performance functional molecular devices, but also facilitates the exploration of fundamental physical and chemical processes.

Ionic liquids are formed by pure ions, which is the basis of its response to an electric field [69,70]. Applying an electric field to the gate in single-molecule junctions with ionic liquid, the ionic liquid will form an EDL structure, like a capacitor that holds a large amount of charge [59,71,72]. The formed electric field then apply to single-molecule junctions, which changes the position of the orbital energy level of the molecule, thus achieving the regulation of the molecular conductance, and enabling the construction of functional devices [73]. To select a suitable ionic liquid, it is necessary to consider its EDL structure, which is related to the size and structure of ions in the ionic liquid [74,75]. For example, imidazolium-based ionic liquids feature large and bulky imidazolium cations (with a diameter of 1 nm that including side chain length) [76], which can form a densely packed layer at the electrode interface and leads to a relatively thick EDL structure [75]. In contrast, quaternary ammonium-based ionic liquids contain smaller quaternary ammonium cations, which result in a less dense and thinner EDL compared to imidazolium-based ionic liquids [77]. Anions and cations have different sizes, and the application of bias voltage in different directions may lead to a change in the EDL structure, forming an uneven distribution of

Table 1
Typical ionic liquids used in single-molecule junctions.

Ion liquid type	Structure	Decomposition temperature (°C)	Dielectric constant (F/m)	Melting point (°C)	Electrochemical window (V)	Reference
Imidazole		354	5.2	17	5.3	[60,61]
		361	13.1	−71	4.6	[61,62]
		458	11.1	−69	5.5	[63,66]
Quaternary ammonium		390	14.5	−93	3.0	[67,68]

the electric field [78]. Generally, the ionic liquids with the matching volume of anion and cation are more suitable for single-molecule regulation, because their EDL structure has uniform charge distribution and high symmetry under different electric fields. Take [DEME]$^+$[TFSI]$^-$ as an illustrative example, with [DEME]$^+$ having an ionic diameter of ~0.75 nm and [TFSI]$^-$ having an ionic diameter of ~0.72 nm [77]. The resulting electric field demonstrates commendable symmetrical behaviors under different bias directions.

The electrical stability of ionic liquids should also be considered. Excellent electrical stability means that ionic liquids can withstand strong electric fields without deterioration and redox reactions. The electrical stability of ionic liquids can be expressed by the value of their electrochemical window which is the maximum voltage that an ionic liquid can withstand without electrochemical decomposition [79,80]. The wider the electrochemical window is, the higher the total potential of anions and cations in ionic liquid at a certain potential [79]. The ionic liquids with a wide electrochemical window can provide a wider range of electric field modulation to the system, which is conducive not only to the discovery of richer molecular information, but also to the construction of high-performance electronic devices. Previous studies show that cyclic quaternary ammonium salts exhibit pronounced electrochemical stability [81]. In particular, salts containing N,N-propylmethylpyrrolidinium cations demonstrate a broader electrochemical window in cyclic and adipose systems compared to 1-butyl-3-methylimidazolium salts [80]. For aromatic ionic liquids, the presence of vacant π^* orbitals generally enhance the likelihood of reduction reactions [82]. It is shown that imidazolium salts generally exhibit larger reduction potentials than pyridyl cations, although their antioxidant capacity is relatively weak [83–85]. When the anions are the same, increasing the chain length of the cation, such as the side-chain length of the N-alkyl-N-methylpyrrolidinium cation, can also improve the chemical stability of ionic liquids [86]. The increase of alkyl chain length can also enhance the shielding effect of positively charged nitrogen and stabilizes pyrrolidinium ring by reducing its free energy, thus improving its cathode stability [86,87]. In addition, [PF$_6$]$^-$ exhibits superior oxidation stability relative to [BF$_4$]$^-$ due to the presence of more highly electronegative fluorine atoms within [PF$_6$]$^-$, resulting in an elevation in the oxidation potential of approximately 1.0 V [88]. In contrast, ionic liquids containing ions that are easily oxidized have low electrical stability [89]. Halogen ions (does not include fluorine) are easily oxidized, so ionic liquids containing halogen ions usually have a narrow electrochemical window [89].

The electrochemical window of ionic liquids is also related to the measurement environment, such as work function of the electrode and impurities [90–92]. Notably, the presence of impurities, particularly water molecules, can significantly impact this window's breadth. When water is present, the water itself can undergo electrolytic reactions, ultimately leading to a narrowing of the electrochemical window of the ionic liquid [92]. Hence, it is imperative to ensure thorough drying of both the ionic liquids and devices to prevent any secondary reactions triggered by water ingression during the measurements. Despite the myriad factors that may influence and limit the stability and applicability of ionic liquids, it is worth noting that these liquids possess inherent structural tunability [26]. Through deliberate modification of anions and cations, the properties of ionic liquids can be precisely tailored, rendering them highly amenable for investigation within the field of single-molecule regulation.

In the study of single-molecule devices utilizing ionic liquids, extending the operating temperature range is crucial for gathering comprehensive data [6,93]. This requires ionic liquids to withstand a wider temperature range, involving two critical aspects: 1) enhanced temperature tolerance, and 2) low freezing point. Enhanced temperature tolerance, exemplified by the thermal decomposition temperature of ionic liquids, is obviously affected by the structural composition of anions and cations. The stronger interaction between anions and cations results in higher thermal decomposition temperature. For example, for thiazolium-based ionic liquids, the thermal decomposition temperature of the ionic liquid with [NTf$_2$] as an anion is ~350 °C, which is higher than that of the difluoro(oxalato)borate anion (~270 °C) [94]. At lower temperatures, molecular thermal vibrations and the resulting scattering are reduced. This facilitates the exploration of intrinsic electronic properties, chemical reactions, and quantum effects of molecules. For example, it is found that π−π stacking pyrene can enhance ferromagnetic interactions in [NBPBI]$^+$[FeCl$_4$]$^-$ and [PNBPBI]$^+$[FeCl$_4$]$^-$ [95]. In order to realize the effective low temperature measurement of single molecule devices with ionic liquids, the used ionic liquids are required to have a sufficiently low freezing point. The smaller the ionic radius, the stronger the electrostatic attraction between ions, and the lower the freezing point of ionic liquid.

2.2.2. Electric double-layer structure arising from ionic liquids

Ionic liquids manifest an EDL structure at the solid/liquid interface when subjected to an electric field, and this phenomenon determines their role in regulating single-molecule junctions. In this section, we first introduce the theoretical model of the EDL based on traditional electrolytes, and then focus on explaining the formation mechanism and theoretical model of EDL based on ionic liquids.

The theoretical models of EDL structures for traditional electrolytes have undergone significant development over time [71]. Helmholtz pioneered the construction of the EDL model, depicting a neatly arranged distribution of positive and negative ions on each side of the interface, akin to the charge distribution in a plate capacitor (Fig. 2a) [96]. To account for thermal motion, this model evolved into the diffused double layer model. In this revised model, counter ions are subject to electrostatic attraction and thermal motion, leading to their diffusion in the solution when equilibrium is reached [97,98]. Subsequent refinements were made in Gouy-Chapman-Stern model by considering van der Waals force adsorption and ion volume [99]. In the Gouy-Chapman-Stern model, the EDL structure at the solid/liquid interface comprises two distinct
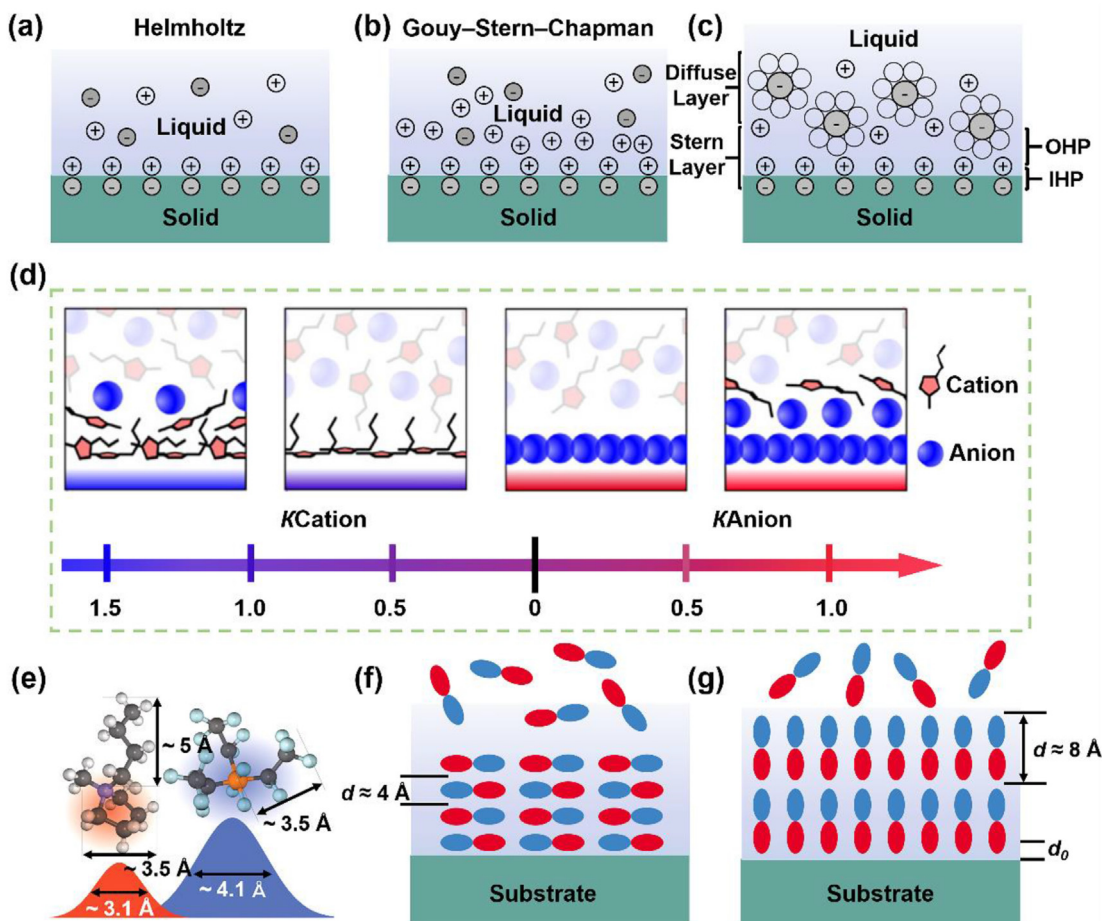
Fig. 2. Electric double layer model of traditional electrolytes and ionic liquids. (a) Schematic of Helmholtz model. (b) Schematic of the Gouy-Chapman-Stern model. (c) Schematic of the EDL structure with the solvent effect. (d) Schematic overview of ion arrangements as a function of normalized positive and negative surface charge density from molecular dynamics simulations (reprinted with permission from Ref. [107] Copyright 2014 Elsevier B.V.). (e–g) The observation of ionic liquid's EDL structure in experiments (reprinted with permission from Ref. [109] Copyright 2008 American Association for the Advancement of Science).

regions: the Stern layer in proximity to the electrode surface and the diffuse layer slightly removed from the electrode surface (Fig. 2b) [99,100]. The electrostatic potential within this model changes linearly in the compact layer and then exponentially in the diffusion layer. Furthermore, Grahame introduced the solvation effect, distinguishing between the adsorption of bare and solvated ions [101]. Consequently, the Stern layer is subdivided into two components: the inner Helmholtz layer (IHP) and the outer Helmholtz layer (OHP) (Fig. 2c) [102]. The inner layer serves as the adsorption region for bare ions, while the outer layer accommodates solvated ions.

The core idea of the classical theory is to exactly calculate the structure of the EDL in equilibrium, relying on the principles of thermodynamics and electrostatics [102]. However, when applied to ionic liquids, this theory encounters added complexity compared to its application in dilute electrolyte solutions. Ionic liquids introduce unique challenges as many of the fundamental assumptions underlying the classical theories do not hold. For instance, ions within ionic liquids often possess larger sizes and exhibit significant charge delocalization, preventing them from being treated as point charges

[102−104]. In addition, the repulsive forces between ions of the same charge become considerably more pronounced in the context of ionic liquid environments compared to dilute solutions. In essence, the EDL structure in ionic liquids is considerably more intricate than that described by the traditional EDL model.

To describe the EDL structure of ionic liquids, the volume occupied by ions needs to be considered. Specifically, ions within ionic liquids are positioned within a relatively fixed lattice at the electrode/liquid interface [105]. Notably, the EDL structure in ionic liquids exhibits a strong correlation with the electrode potential [106]. When the electrode surface maintains a low potential, the response of the ionic liquid to an increase in electrode potential primarily concentrates near the electrode surface, affecting only a layer of counter ions [107]. When the potential of electrode surfaces is high, sufficient counterions need to accumulate at the interface to shield the high surface charge [107]. However, due to the maximum allowable local ion concentration and electrostatic interactions between ions, a multilayer accumulation of the anions and cations in ionic liquids will be formed at the interface, featuring oscillatory attenuation [108]. The response of the

EDL structure of ionic liquids to the potential of electrode surfaces is shown in Fig. 2d [107]. Experimental observations align with the theoretical calculations, revealing that the EDL structure of ionic liquids can extend beyond a few nanometers into the liquid, surpassing a single ionic layer's thickness [109–111]. For instance, distinct alternating layers of ions become evident when measuring the reflection from substrate surfaces coated with ionic liquids (Fig. 2e–g) [109].

2.2.3. Construction of single-molecule junctions within ionic liquids

In this section, we provide an overview of the two-electrode, three-electrode, and four-electrode systems within ionic liquids, with a particular emphasis on their role in single-molecule junctions.

For two-electrode system, there are only two electrodes, and no reference electrode and opposite electrode (Fig. 3a) [112]. The electrochemical control effect is achieved through the two working electrodes: tip and substrate. For example, it is found that the molecular rectification in polar solvents after the gold tip is encapsulated, because the asymmetric exposure of ionic liquids around tip and the untreated flat substrate produces an asymmetric EDL structure. The asymmetry of electrode pairs opens a new way to adjust single-molecule devices by ionic liquids.

Furthermore, a three-terminal single-molecule device is created by introducing a gate into single-molecule junctions, which regulates the electronic behavior through the field effect [73,113]. In dynamic junctions, for instance, when a positive voltage is applied to these platinum counter-electrodes, the working electrode generates a corresponding negative voltage. Subsequently, the negatively charged working electrode attracts cations from the ionic liquid, leading to the formation of an EDL at the electrode interface. This EDL, in turn, generates an electric field, effectively regulating the carrier transport behaviors in single-molecule junctions (Fig. 3b) [113]. In static junctions, such as graphene point electrode systems, the gate electrode is typically fabricated onto the device through micro-nano machining techniques, followed by the introduction of the ionic liquid (Fig. 3c) [73]. Similar to dynamic junctions, the application of a gate voltage prompts the ionic liquid to form an EDL structure. The resulting gate electric field can then regulate the alignment between the molecular frontier orbital and the Fermi level of the graphene electrode, thereby fine-tuning the charge transport characteristics of the junctions.

An Ag/AgCl reference electrode is further introduced into the three-electrode dynamic junctions to construct a four-electrode system, which is regulated by electrochemical principle (Fig. 3d) [114]. The four-electrode system affords separate control over the potential applied to the working electrode and the bias between the tip and the base. This separation ensures that adjustments to the working electrode's potential can be made without altering the bias. The introduction of the reference electrode significantly diminishes the influence of electrode polarization and solution IR drop, resulting in more precise control over the working electrode's potential. Moreover, within the four-electrode system, all the potential applied to the working electrode is dedicated to regulating the electrode's energy level, yielding exceptionally high regulation efficiency.
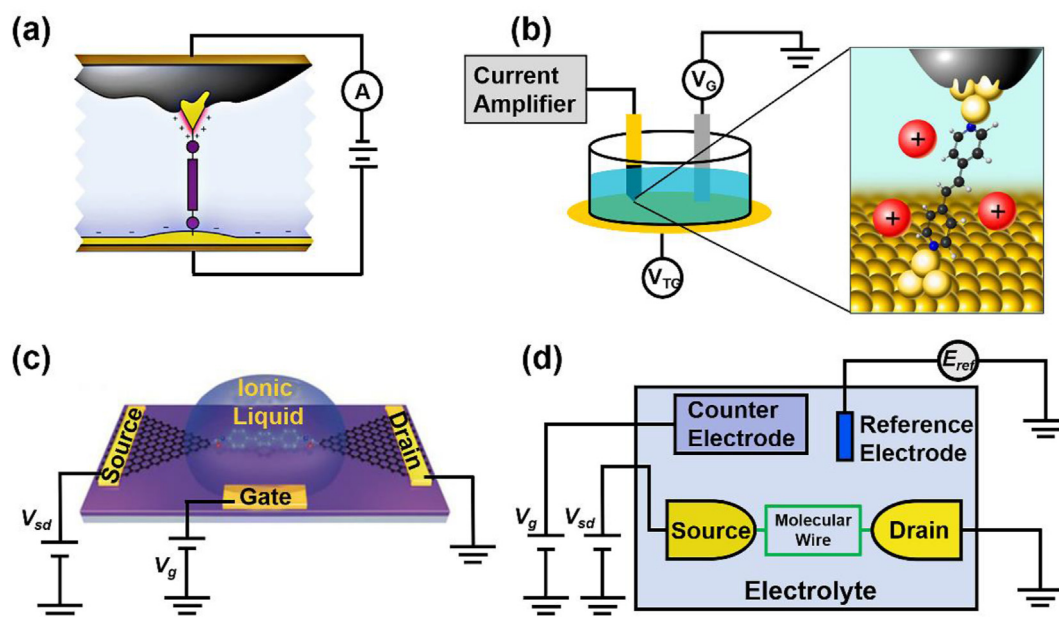

Fig. 3. introduction of ionic liquids in single-molecular devices. (a) Two-electrode system (reprinted with permission from Ref. [112] Copyright 2015 Macmillan Publishers Limited). (b) Dynamic junction systems with three electrodes (reprinted with permission from Ref. [113] Copyright 2014 American Chemical Society). (c) Static junction systems with three electrodes (reprinted with permission from Ref. [73] Copyright 2018 Wiley-VCH Verlag GmbH & Co. KGaA, Weinheim). (d) Four-electrode system (reprinted with permission from Ref. [114] Copyright 2016 American Chemical Society).

3. Role and regulation mechanism of ionic liquids in single-molecule junctions

Understanding the role and regulation mechanisms of ionic liquids in single-molecule junctions is essential for both uncovering fundamental device principles and advancing innovative functional devices. This chapter firstly introduces the mechanism of ionic liquids as a dielectric layer to provide gate voltage control, then explains how ionic liquids serve as electrolytes to achieve electrochemical control, and finally clarifies how ionic liquids act as ions to change the structure of the interface to regulate charge transport in the device.

3.1. Gate control

One primary role of ionic liquids in single-molecule junctions is to serve as dielectric layers, enabling gate regulation and consequent modulation of energy levels [59,73,115]. The ideal gate regulation should adhere to the following key criteria: (1) Proximity between gate and molecule: to maximize efficiency, the distance between the gate and the molecule should be minimized [93]. This proximity ensures that the gate's electric field can directly and effectively influence the molecule's behavior. (2) High electrostatic coupling strength: it is essential to achieve a high electrostatic coupling strength between the gate electrode and the molecular frontier orbitals, such as HOMO and LUMO. This coupling strength can be quantified using the electrostatic coupling parameter ξ. A higher ξ value signifies a stronger coupling between the applied gate voltage and the molecular frontier orbitals, resulting in more efficient modulation of these orbitals by the gate [116]. (3) High dielectric constant of the dielectric layer: the dielectric layer's dielectric constant, also known as its permittivity, should be sufficiently high. A higher permittivity enhances the ability of the dielectric layer to accumulate induced charge on its surface in response to an applied gate voltage. This accumulation generates a stronger electrostatic field, amplifying the effective gate voltage and, in turn, its impact on the molecule. (4) Mitigate source-drain shielding effect: It is crucial to minimize the shielding effect of the source-drain configuration on the gate electric field [93]. This effect is associated with both the length of the gap between source and drain electrodes and the distance between the gate electrode and the molecule. The shielding effect becomes more pronounced when the distance between the gate and the molecule exceeds the distance between the source and the drain [73].

In this context, ionic liquids are particularly well-suited for meeting the aforementioned requirements. Specifically, ionic liquid gates have natural advantages: (1) Effective application of gate electric field: the gate electric field can be effectively applied to the single molecules [59,93]. When a gate voltage is applied, the ionic liquid will form an atomically thick EDL structure at the electrode/molecule interface, thus ensuring the effective application of the gate electric field on the molecules. For instance, experimental measurements reveal that $[bmpy]^+[FAP]^-$, a representative ionic liquid, has an EDL thickness of ~8 Å, which is significantly thinner than solid gates (5 nm) [109]. (2) High dielectric constants: Ionic liquids exhibit extremely high dielectric constants for gating, compared to other traditional solid-state dielectric materials such as SiO_2 (with a dielectric constant of ~3.9). For example, $[DEME]^+[TFSI]^-$, a commonly used ionic liquid gate in single-molecule devices, boasts a dielectric constant of ~14.5 [68]. Other ionic liquids commonly used in single-molecule devices also possess high dielectric constants. For instance, 1-butyl-3-methylimidazolium trifluoromethanesulfonate has a dielectric constant of ~5.1, while 1-hexyl-3-methyl-imidazolium hexafluoro phosphate and 1-butyl-3-methyl-imidazolium hexafluorophosphate have dielectric constants of ~11.1 and ~13.1, respectively [60,66]. The use of ionic liquids as the dielectric layer can significantly enhance the gate control performance of the device. (3) Mitigation of gate shielding effect: Ionic liquids offer the advantage of avoiding gate shielding effects. The thickness of the ionic liquid double-layer structure depends on the ion size, allowing for the selection of an appropriate ionic liquid based on the length of the molecular bridge [74,75]. This reduces the impact of source and drain electrodes on shielding the gate electric field. These characteristics make ionic-liquid gate a valuable choice for precise control and regulation in single-molecule junctions.

The regulation mechanism of an ionic liquid gate is the same as that of traditional solid gate, which is affected by the molecule/electrode coupling strength and the relative position of molecular orbital energy level and the electrode Fermi level. The interfacial coupling strength is an important factor determining the transport mechanism of single-molecule junctions. In the strong coupling regime, the electron states of the molecule and electrode significantly overlap, leading to partial charge transfer between the molecule and the electrode [117,118]. This interaction results in a considerable broadening of the molecular energy levels. Under strong coupling conditions (Fig. 4a), electrons can efficiently traverse from one electrode to another through a one-step coherent process, with minimal interaction with the molecule itself [118]. In the intermediate coupling regime (Fig. 4b), the molecular energy levels experience partial broadening. Here, the electron transfer process is influenced by the electron state of the molecule [118]. Molecules possessing lone pair electrons can have their spin states altered by the transferred electrons. Moreover, resonant tunneling becomes feasible in this state, where an electron tunnels into the LUMO of the molecule while another electron simultaneously tunnels out from the HOMO. This leaves the molecule in an excited state. Under conditions of weak coupling (Fig. 4c), the interaction between charges and molecules is pronounced, resulting in primarily incoherent electron transport [118]. In this mode, electron transport occurs in two discrete steps: firstly, electrons jump from the source electrode to the molecule, and subsequently, they hop from the molecule to the drain electrode, surmounting an activation barrier in the process. In weak coupling scenarios, Coulomb blockade phenomena may manifest when the energy levels of the molecule and the electrode fail to align
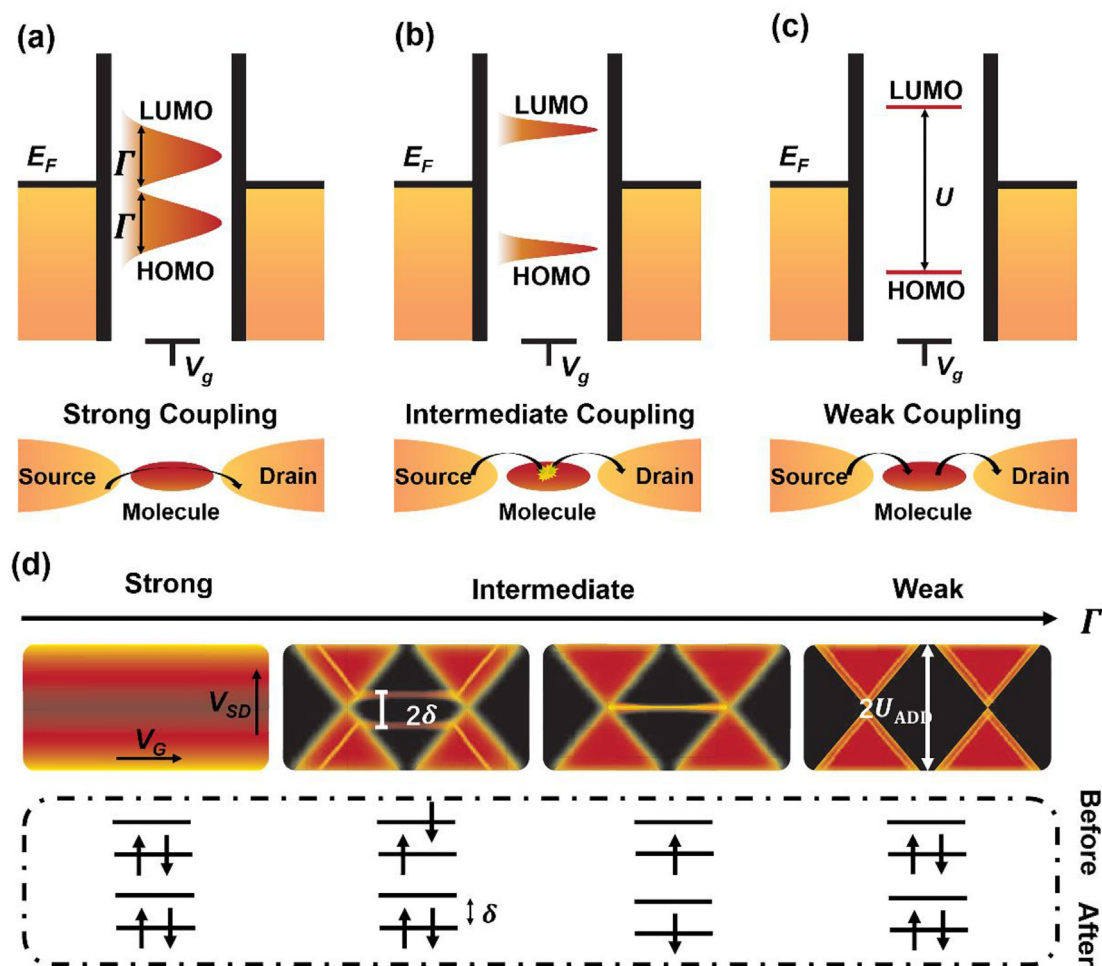
Fig. 4. Schematic diagram of molecular energy levels and charge transport processes of single-molecule junctions at different molecular/electrode coupling strengths: (a) strong coupling state, (b) intermediate coupling state, and (c) weak coupling state. (d) Charge transport at different coupling strengths in a three-terminal device. (Fig. 4 reprinted with permission from Ref. [118] Copyright 2022 American Chemical Society).

(Fig. 4d) [119]. This misalignment hinders electron transport and is prominently observed through characteristic Coulomb diamonds in differential conductance mappings. Conversely, strong coupling conditions disrupt the Coulomb blockade effect, diminishing the influence of gate voltage on charge transport (Fig. 4d). These coupling regimes govern the diverse electron transport behaviors encountered in single-molecule junctions, shaping their fundamental properties and performance characteristics.

When a gate voltage is applied, the ionic liquid forms an EDL structure, giving rise to a gate electric field. This electric field, when exerted on the single-molecule junction, has the capability to adjust the relative energy position of the molecular orbital in relation to the Fermi level of electrodes [6,35]. This adjustment subsequently leads to alterations in the electron transport behavior within the single-molecule devices. Taking the single-molecule junctions composed of aromatic molecules and graphene electrodes as an example, both experimental and theoretical investigations confirm that the introduction of ionic liquid gates can effectively modify the orbital energy levels, thereby adjusting the charge transport characteristics (Fig. 5a) [73]. As shown in Fig. 5b, when the applied gate voltage is positive, the molecular orbital energy level shifts downward relative to the Fermi level. Thus, the molecular HOMO moves away from the Fermi level, while LUMO approaches the Fermi level [73]. Conversely, the reverse adjustments occur when the applied gate voltage becomes negative.

When there is a similar length between the molecular length and the EDL size of the ionic liquid, ionic liquid gates will influence the charge transport of molecular devices through the screening effect. Biphenyl molecular junctions display a contrasting gate voltage dependence compared to terphenyl and hexaphenyl molecular junctions [73]. The conductivity of biphenyl molecular systems decreases as the gate voltage transitions from negative to positive. In contrast, for terphenyl and hexaphenylbenzene molecular systems, the conductivity initially decreases and then increases as the gate voltage shifts from negative to positive, with an inflection point at approximately 0.5 V. This peculiar behavior of biphenyl molecular junctions can be attributed to a gate shielding effect arising from the similarity in the molecular length (approximately 9.9 Å) and the size of the ionic liquid EDL (approximately 7.5 Å).
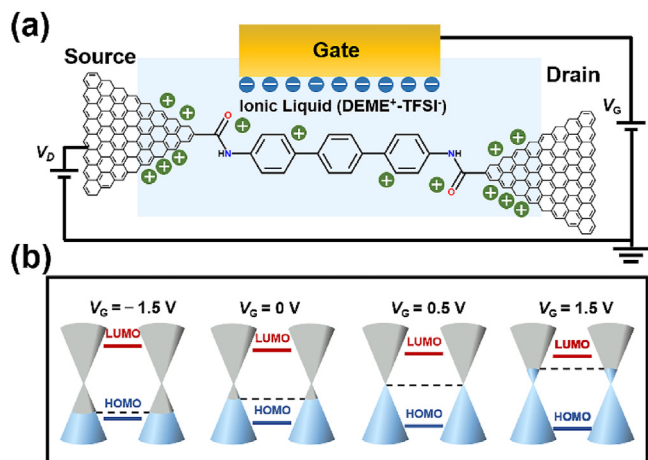
Fig. 5. Gate regulation mechanism of single-molecule devices with an ionic liquid gate. (a) Single-molecule junctions composed of aromatic molecules and graphene electrodes. (b) Schematic of molecular orbital energy level controlled by an ionic liquid gate (Fig. 5 reprinted with permission from Ref. [73] Copyright 2018 Wiley-VCH Verlag GmbH & Co. KGaA, Weinheim).

3.2. Electrochemical control

Ionic liquids can act as electrolytes to achieve electrochemical control and thus regulate the molecular redox reactions in single-molecule junctions. According to whether there is redox reaction, the potential interval in the cyclic voltammetry curve of the molecule can be divided into non-Faraday interval (no occur) and Faraday interval (redox occur) [120]. The regulatory mechanisms of ionic liquids are different in different regions. When applying potential of non-Faraday interval in the range of molecules, the molecular redox reaction cannot occur [120]. At this time, the modulation mechanism of the ionic liquid is the same as that in 3.1, providing gate voltage regulation as the dielectric layer.

In Faraday potential range, electrons are transferred from one electrode to the molecule and then from the molecule to the other electrode, and this process is called two-step hopping (Fig. 6a) [116,121]. During the process, electrons interact strongly with individual molecules, triggering a redox reaction that may change the molecular conductance. In general, the maximum conductance of the single-molecule junction with a redox active center is located at the proper bias window (Fig. 6b) [122]. Specifically, when the molecular energy level shifts within the chemical potential windows of the two electrodes, a resonant conductive state that significantly boosts the conductance of the molecular junction is created. Conversely, as the molecular energy level moves outside of these windows, the conductance proportionally diminishes.

The conductance of a single-molecule junction with a redox active center varies with changes in potential. This dynamic behavior is influenced by a confluence of parameters, among which the shift in the effective electrode potential occurring at the redox center due to variations in bias voltage (denoted as γ), as well as the fraction of the electrochemical potential manifested at the redox site (designated as ξ), assume critical

roles in modulating said conductance [123]. In comparison to traditional electrolyte systems, the γ for the ionic liquid is very small, and ξ is approximately equal to 1 [122]. This implies that in ionic-liquid electrochemical-gating systems, the bias effect contributes much less than the potential effect to the modulation of the molecular junction redox center. Fig. 6c and d show the conductance curves of molecular junctions as they change with electric potential in ionic liquids and aqueous environments, respectively. It has been demonstrated that in ionic liquid environments, the viologen junction conductance exhibits a bell shape in response to potential variations (Fig. 6c) [124]. Conversely, in an aqueous solution, the viologen molecular junction displays continuous and monotonic changes with potential, primarily due to the relationship between γ and ξ, which broadens the "bell-shaped" peak. Furthermore, the narrow potential window of the aqueous solution limits its ability to provide a comprehensive view of the bell shape, resulting in monotonic changes (Fig. 6d) [124]. This implies that ionic liquids enable a more comprehensive representation of charge transfer processes and achieve higher efficiency in electrochemical regulation.

Ionic liquids exhibit high gate coupling efficiency with molecules, facilitating the acquisition of intricate charge transfer processes. For instance, in ionic liquid systems, fine-tuned redox processes can be observed by adjusting the length of the chain connecting the redox center to the electrode surface. In single-molecule junctions involving the Fc center with alkane chain linking to the electrodes, the electronic interaction between the redox Fc center and the electrode decreases with the increase of alkane length, thus altering the rate of electron transfer between the electrode and the molecule (Fig. 6e) [125]. With an increasing molecular length, a significant rise in the frequency of switching events between high and low conductance states becomes evident.

3.3. Molecule-electrode interface control

Ionic liquids can also act as ions to modulate charge transport in single-molecule junctions by affecting the structure of molecule-electrode interfaces. The ionic liquid can be adsorbed on the electrode surface and change the molecular adsorption configuration to regulate the charge transport characteristics [126,127].

For instance, it has been found that the electronic interaction at the interface, induced by the adsorption of 1-butyl-3-methylimidazolium (BMI) cations on Au (111), can impede the coupling between the π bond of the pyridine ring and the Au electrode while enhancing the coupling between the σ bond of the terminal N atom and the Au electrode (Fig. 7a) [126]. Consequently, in the presence of BMI cation, the predominant adsorption configuration of 4,4'-BPY is vertical through the σ bond, rather than the planar adsorption configuration via the π bond. This leads to significant alterations in the charge transport characteristics of the single molecule (Fig. 7a−c). Upon the introduction of water molecules into the system, the BMI groups adsorbed on the Au electrode surface are displaced by water molecules, causing
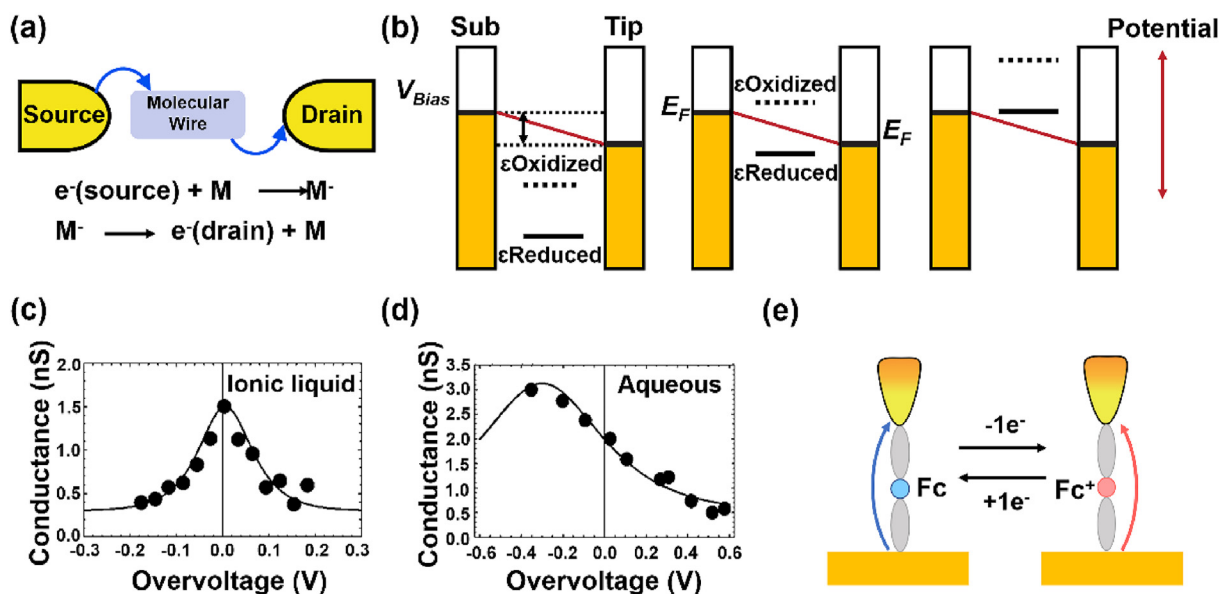
Fig. 6. The electrochemical regulation mechanism of single-molecule devices with ionic liquids. (a) Schematic diagram of electron transfer in Faraday potential range (reprinted with permission from Ref. [121] Copyright 2022 IOP Publishing Ltd). (b) Schematic diagram of the conductance of the single-molecule junction with a redox active center as a function of potential (reprinted with permission from Ref. [122] Copyright 2012 American Chemical Society). (c) Single-molecule conductance and potential data in ionic liquids. (d) Single-molecule conductance and potential data in aqueous. ((c) and (d) reprinted with permission from Ref. [124] Copyright 2015 American Chemical Society). (e) Schematic diagram of charge transport of a single molecule with Fc unit (reprinted with permission from Ref. [125] Copyright 2019 National Academy of Sciences).

the 4,4′-BPY molecules to revert to a tilted adsorption configuration on the Au surface (Fig. 7d). These modifications in single-molecule conductance provide clear evidence of the transition in the pyridine adsorption configuration (Fig. 7e and f).

In addition, different counter-ionic environments also have an impact on the molecular structure. For example, counterions determine the twist angle between the pyridine-pyridine ring and the phenyl-pyridine ring [128]. The interaction between ionic liquids and single-molecule junctions has been
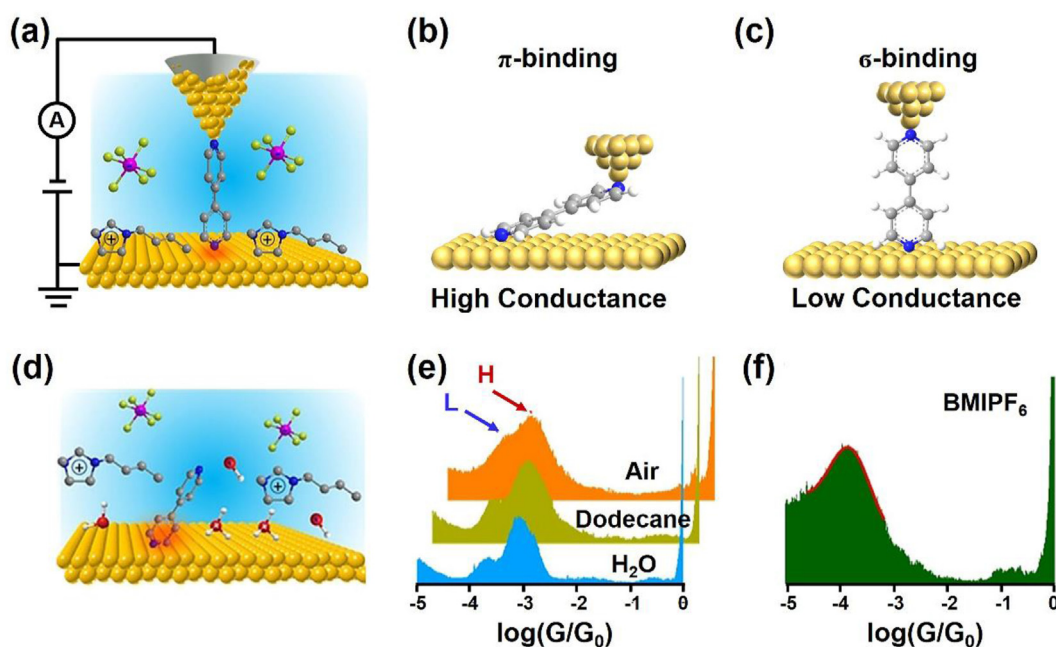

Fig. 7. The molecule-electrode interface regulation mechanism of ionic liquids. (a) Schematic diagram of BMI adsorption on the Au electrode surface. (b, c) Diagram of different 4,4′-BPY binding configurations. (d) Water molecules adsorb on the surface of the Au electrode surface. (e) Conductance of 4,4′-BPY molecular junctions in aqueous solution. (f) Conductance of 4,4′-BPY molecular junctions in ionic liquids. (Fig. 7 reprinted with permission from Ref. [126] Copyright 2021 Wiley-VCH Gmb).

confirmed to be one of key factors affecting the charge transport, providing a new approach for the effective and versatile utilization of ionic liquid in single-molecule junctions.

4. Application of ionic liquids in single-molecule junctions

Single-molecule device research is primarily oriented towards two critical avenues: device functionalization and the pursuit of innovative physicochemical mechanisms enabled by these devices. Ionic liquids, owing to their remarkable attributes encompassing a wide electrochemical window, low volatility, exceptional thermal stability, and robust design flexibility, wield a profound influence, significantly enhancing investigations in both these dimensions. This influence manifests in the advancement of high-performance electronic devices founded upon ionic liquids, exemplified by quantum interference devices. Moreover, ionic liquids find application as regulators of chemical reactions within single-molecule devices, underlining their critical role in facilitating sophisticated control at the molecular level.

4.1. Developing high-performance functional devices

Ionic liquids can serve as gate dielectrics in single-molecule field-effect transistors (FETs) with quantum interference effects to effectively control the charge transport and achieve high performance. Two primary types of quantum interference effects, known as constructive quantum interference (CQI) and destructive quantum interference (DQI), lead to unique conductivity properties [116]. Molecules featuring the CQI effect exhibit significantly enhanced conductivity behavior, resulting

in higher on-state current in single-molecule junctions. On the other hand, molecules with the DQI effect have transmission spectra that sharply decrease near the Fermi level. Consequently, single-molecule junctions with the DQI effect display lower off-state current.

By adjusting the electrode potential of the ionic liquid gate, it is possible to modulate the energy level of molecules with quantum interference effect to the anti-resonance state. This allows for the direct observation of sharp DQI characteristics due to changes in the relative positions of molecular energy levels, all without altering the molecular redox state. For example, the DQI effect of *meta*-benzene-based molecule with dihydrobenzo[b]thiophene as the anchoring group (*meta*-BT) can be controlled by the electrode potential of 1-butyl-3-methylimidazolium hexafluorophosphate (BMIPF$_6$) (Fig. 8a) [129]. At a gate potential of -0.4 V, the molecular conductivity is two orders of magnitude lower than when the gate potential is 0 V, mainly due to the DQI effect (Fig. 8b). Similarly, the junction of 2,4-TP-SAc with DQI can also be controlled by an ionic liquid gate (Fig. 8c) [53]. In the potential range of -0.6 V to -0.4 V (vs. Ag/AgCl) and -0.4 V to 1.4 V (vs. Ag/AgCl), the conductance of the molecular junction firstly decreases and then increases, resulting in an on-off ratio as high as ~100 times (Fig. 8d and e). This demonstrates the feasibility of continuous and efficient regulation of molecules with DQI effects through ionic liquids for the construction of high-performance single-molecule devices.

Besides a single molecule, the monolayers formed by the self-assembly of molecules also have the same quantum interference effect as the basic molecule, which is in favor of constructing efficient and stable quantum tunneling field-effect devices. For example, using pseudo-p-bis((4-(acetylthio)
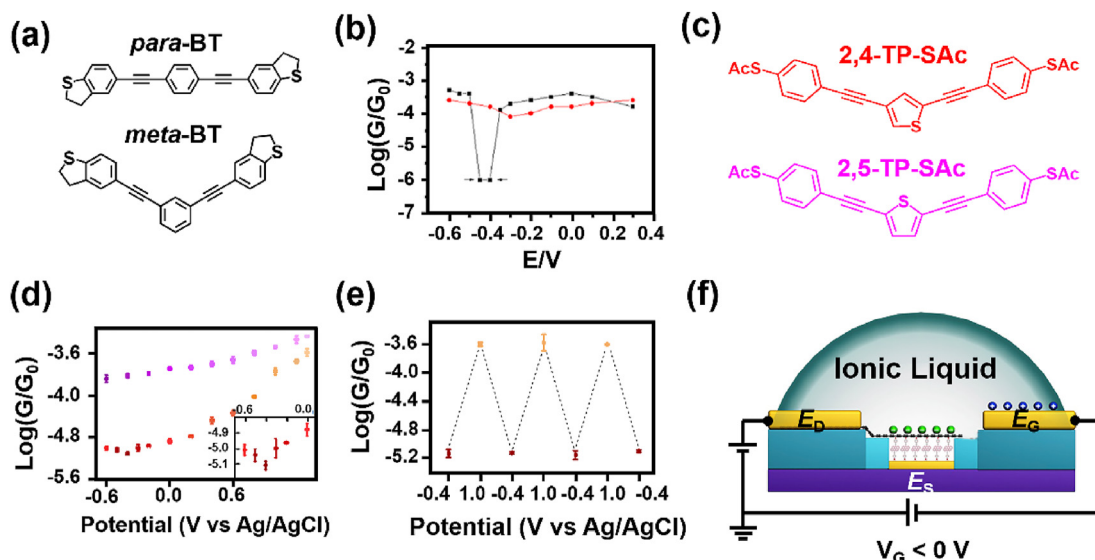

Fig. 8. Improved switching ratio based on quantum interference effect. (a) Chemical structures of *para*-BT and *meta*-BT molecules. (b) The molecular conductance changes of para-BT and meta-BT molecules versus electrode potentials. ((a) and (b) reprinted with permission from Ref. [129] Copyright 2018 American Chemical Society). (c) Chemical structures of 2,5-TP-SAc (purple) and 2,4-TP-SAc (orange). (d) The molecular conductance changes of 2,5-TP-SAc (purple) and 2,4-TP-SAc (orange) versus electrode potentials. (e) Reversible switching of 2,4-TP-SAc. ((c–e) reprinted with permission from Ref. [53] Copyright 2018 Springer Nature). (f) Schematic illustration for the setup of the device with a vertical ionic liquid gate (reprinted with permission from Ref. [131] Copyright 2018 Elsevier Inc).
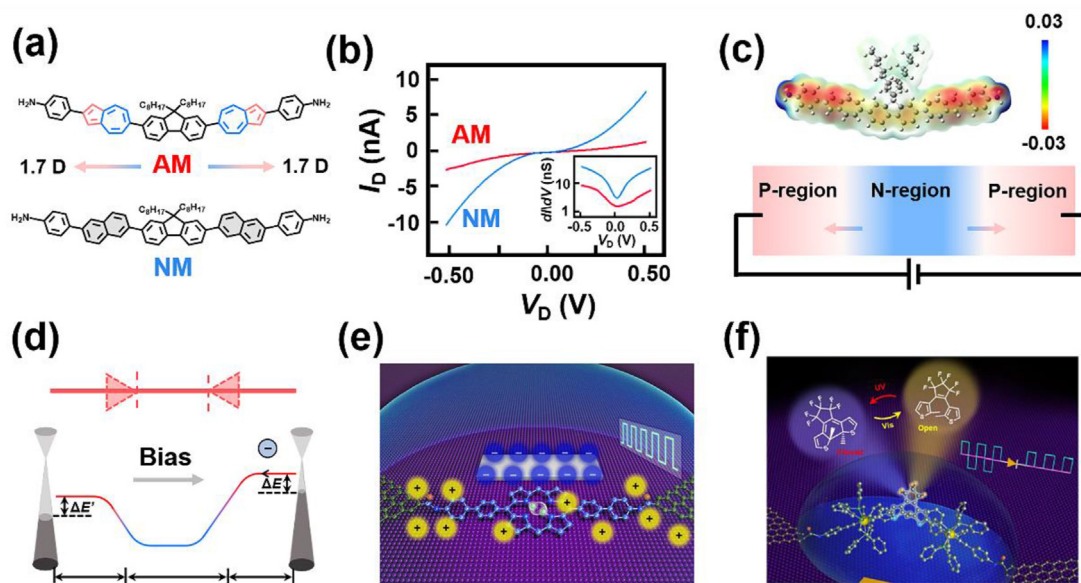
Fig. 9. Improved switching ratio based on other strategies. (a) Chemical structures of AM and NM molecules. (b) Experimental *I–V* characteristics for AM-based single-molecule junctions and NM-based single-molecule junctions. ((a, b) reprinted with permission from Ref. [132] Copyright 2022 The Royal Society of Chemistry). (c) Schematic diagram of the PNP structure in the AM-based single-molecule junction. (d) Schematic diagram of the charge transport of AM-based molecule junctions. ((c, d) reprinted with permission from Ref. [133] Copyright 2022 American Chemical Society). (e) Schematic of a graphene-porphyrin-graphene junction (reprinted with permission from Ref. [134] Copyright 2022 American Association for the Advancement of Science). (f) Schematic of graphene-Ru-DAE-graphene junctions (reprinted with permission from Ref. [135] Copyright 2021 American Chemical Society).

phenyl)ethynyl)-p- (2,2) cyclophane (PCP) with destructive quantum interference effects (DQI) to create vertical molecular tunneling field-effect devices with an ionic liquid gate, achieving an on-off current ratio of ~330 [130]. In addition, the anthanthrene nucleus molecules with DQI effects can also be used to construct vertical tunneling devices (Fig. 8f) [131].

In addition to quantum interference effects, the creation of high-performance single-molecule functional devices can be achieved by combining various molecular properties with ionic liquid gate control. When the structure of a single-molecule junction is fixed, enhancing the molecular electric field responses enables a larger switching ratio with a lower gate voltage. For example, in a liquid gate FET, a single-molecule junction containing an azulene center exhibits a higher on/off ratio than a molecular device containing a naphthalene center (Fig. 9a) [132]. This is because molecules containing the azulene center possess higher dipole moments, resulting in reduced leakage current (the current when the Fermi level is between the HOMO and LUMO orbitals). Consequently, this enhances the on/off ratio (Fig. 9b).

Moreover, the intrinsic dipoles within molecules can effectively regulate the charge transport and associated potential barriers in single-molecule junctions. For instance, the azulene-ring molecule, which consists of two units with opposing dipole directions, displays a PNP structure (Fig. 9c) [133]. The presence of dual potential barriers, induced by the double dipole moment, impedes charge transport at the molecular junction and necessitates a turn-on voltage to initiate charge transport (Fig. 9d).

In addition, the design of functional centers or molecules with high conjugation can augment the on-state current. Take porphyrin molecules as an example, their highly conjugated central macrocyclic structure results in a more delocalized electron cloud distribution, enhancing the conductivity and increasing the open-state current of molecular junctions (Fig. 9e) [134].

The construction of devices with rectification functions based on ionic liquids is also expected. In single-molecule photoswitching devices based on dinuclear ruthenium diarylethylene molecules (Ru-DAE), the introduction of ionic liquid $DEME^+$-$TFSI^-$ leads to single-molecule gated rectification. Under visible light irradiation, the diarylethene unit transforms into an open ring state and connects the relatively independent left and right Ru segments. The molecular frontier orbitals of the two segments adjusted to move asymmetrically under the application of a gate field, thereby achieving the rectification function (Fig. 9f) [135].

4.2. Exploring chemical reaction mechanism

Furthermore, ionic liquids have been employed not only to enhance the performance of single-molecule devices, but also to investigate dynamic reactions at the single-molecule level. This includes the precise control of Mizoroki−Heck catalytic reactions, free-radical electrochemical reaction, and electron transfer reactions facilitated by ionic liquid gates [136−138].

The electric field generated by the ionic liquid gate can specifically influence the energy barrier for olefin migration insertion, a rate-determining step in the Mizoroki−Heck reaction (Fig. 10a and b) [136]. The catalytic activity is fine-tuned by this electric field, arising from the EDL structure of the ionic liquid. A more negative gate voltage enhances the rate of the oxidative addition reaction (Fig. 10a), while a more positive gate voltage accelerates the reduction rate of Pd
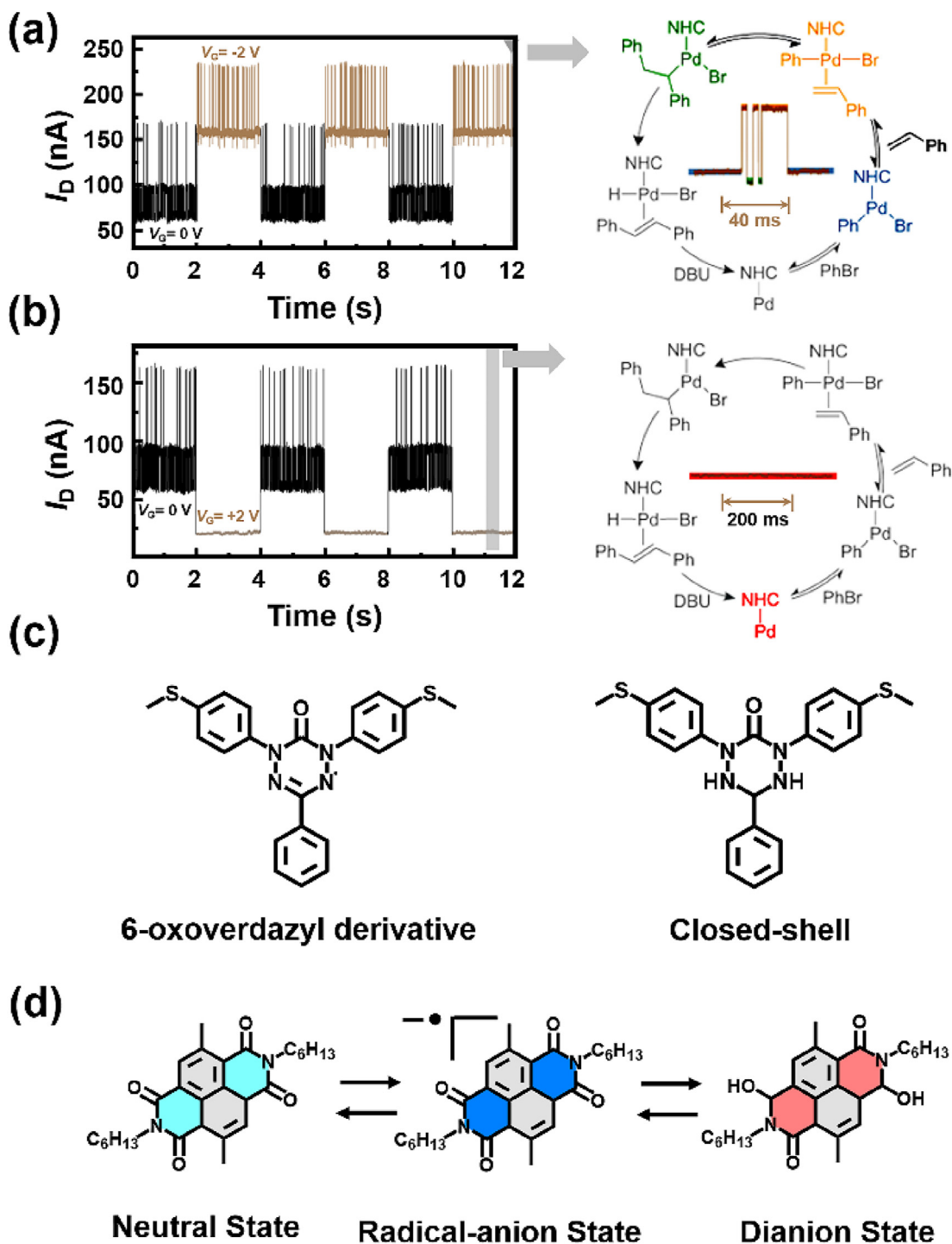
Fig. 10. The application of single-molecule devices with ionic liquids to explore chemical reaction mechanisms. Gate tuning of the single-molecule Mizoroki−Heck reaction upon applying (a) −2 V/0 V gate voltage and (b) +2 V/0 V gate voltage. ((a) and (b) reprinted with permission from Ref. [136] Copyright 2022 Springer Nature). (c) Structures of the 6-oxoverdazyl derivative and corresponding closed-shell structure (reprinted with permission from Ref. [137] Copyright 2022 Wiley-VCH GmbH). (d) Two electron transfer reactions of nuclear-substituted naphthalenediimide (NDI) molecules (reprinted with permission from Ref. [138] Copyright 2015 Wiley-VCH Verlag GmbH & Co. KGaA, Weinheim).

(Fig. 10b). Essentially, the ionic liquid gate adjusts the frontier orbital of the NHC−Pd complex, leading to varied reactivity in the oxidative addition or reductive elimination processes. By modulating the application of the gate voltages during the reaction, the instantaneous initiation or cessation of the Mizoroki−Heck reaction can be observed. Consequently, the

reaction can be precisely controlled using the ionic liquid gate, offering valuable insights for designing innovative single-molecule catalytic reaction pathways.

When a certain gate voltage is applied, the phenomenon of promoting or suppressing the Mizoroki−Heck reaction is observed. By alternately applying these gate voltages during

the reaction, the instantaneous start or stop of the Mizoroki−Heck reaction can be observed, thus achieving control of the reaction through an ionic liquid gate. This provides a good idea for designing new modes of single-molecule catalytic reactions.

Applying a gate voltage via the ionic liquid gate can efficiently manipulate the electrostatic potential of the molecular bridge, inducing single-molecule free radical reactions. For instance, single-molecule junctions of 6-oxoverdazyl radicals, constructed using the STM-BJ method, possess open-shell properties. In the presence of the ionic liquid1-butyl-3-methylimidazolium triflate, free radical compounds can undergo reversible electrochemical reduction, transforming into closed-shell anions and exhibiting distinct charge transport characteristics under these two states (Fig. 10c) [137]. Moreover, ionic liquids can modulate electron transfer reactions. For instance, two electron transfer reactions of core-substituted NDI molecules are successfully regulated by ionic liquid electrochemical control. When the positive charge of the ionic liquid aligns closely with the NDI molecular plane, it facilitates the transfer of electrons from the Au electrode to the molecule, thereby promoting the electron transfer reaction (Fig. 10d) [138].

5. Summary and outlook

In summary, leveraging the unique properties of ionic liquids and their benefits in the realm of single-molecule junctions, this review elucidates the regulatory mechanisms and diverse applications of ionic liquids in single-molecule devices. The combination of ionic liquids with single-molecule technologies opens up numerous possibilities for future catalyst optimization, device development, and advancements of ionic liquids. Here, we outline several critical research topics in this field, aiming to promote the relevant development.

5.1. Exploring catalysis involved ionic liquids at the single-molecule level

By combining single-molecule techniques and ionic liquids, we can delve into understanding reaction and catalysis mechanisms, optimizing catalysts, developing green catalysis, and understanding catalysis in extreme conditions.

Reaction and catalysis mechanisms: A deep understanding of the catalytic activity of ionic liquids at the single-molecule level is essential for promoting the design of more efficient and selective catalysts, which includes: 1) Precise reaction monitoring: Monitoring reactions at the single-molecule level allows for precise tracking of reaction intermediates and product. This can reveal reaction pathways and kinetics that might not be apparent in bulk studies. 2) Identification of active sites: Identifying active sites within ionic liquids and their interactions with reactants, catalysts, and substrates. This can shed light on the mechanism of reaction selectivity in asymmetric catalysis and quantifying reactivity variations among different ionic liquid compositions and structures. 3) Precise reaction control: Single-molecule regulation techniques provide precise control over reactant molecules and catalytic sites at the molecular level. This level of control is especially valuable in understanding and optimizing asymmetric catalytic reactions such as chiral catalysis.

Enhanced catalyst design: High-throughput screening of various ionic liquid-catalyst combinations at the single-molecule level can expedite the discovery of new efficient catalysts. This approach can identify promising candidates for further optimization and scale-up.

Environmental and green catalysis: Ionic liquids are often considered "green" solvents due to their low volatility and recyclability. The combination of ionic liquids and single-molecule junctions can contribute to the development of environmentally friendly and sustainable catalytic processes.

Catalysis in extreme conditions: Ionic liquids, known for their low melting points and stability, can facilitate catalytic reactions at low temperatures. Single-molecule devices can be used to study catalytic mechanisms under these conditions, which may be relevant in certain applications, such as pharmaceutical synthesis.

5.2. Functionalization of single-molecule devices using ionic liquids

Appropriate selection of ionic liquids can be applied to improve the performance of single-molecules devices as well as construct novel devices. The functionalization of single-molecule devices using ionic liquids represent highly promising areas of research at the intersection of electrochemistry and nanotechnology.

Performance improvement of single-molecule functional devices: Fundamentally, selecting an ionic liquid with a low viscosity and high ion mobility can improve the efficiency of electron or hole transfer through the molecule, leading to enhanced device conductivity. The use of cooperative bonding strategies involving multiple ionic liquids or molecules can be investigated to achieve more complex and reversible conductance changes, which could lead to the development of high-performance molecular devices.

Construction of novel single-molecule functional devices: Researchers can explore the design and synthesis of ionic liquids tailored for specific functional device, such as spin filtering and quantum computing devices. For example, chiral ionic liquids can be utilized to introduce spin filtering capabilities into single-molecule devices. Spin-selective interactions between chiral ionic liquids and molecules can lead to the separation of spin-up and spin-down electrons, making it possible to create spintronic devices with enhanced performance. The electric field regulation using ionic liquids provides a versatile approach to achieve spintronic control in single-molecule devices. By manipulating the electric field within the device through the application of ionic liquids, it is possible to modulate the spin properties of the molecules, enabling the creation of novel quantum devices.

5.3. Probing structure and interactions for ionic liquids

The ionic interactions and EDL structures for ionic liquids plays a crucial role in various electrochemical processes. The single-molecule techniques provide a powerful tool to deeply understand these interactions and structures of ionic liquids precisely and dynamically.

Ionic structure effects: Single-molecule techniques can be employed to study how changes in the ionic structure of ionic liquids impact the structure and behavior of the EDL. Different combinations of cations and anions in ionic liquids can lead to variations in the ionic size, charge, and polarizability. Understanding how these structural variations influence the EDL's composition, thickness, and charge distribution is crucial for tailoring ionic liquids for specific applications.

Nanopore-based studies: Building upon nanopore-based single-molecule techniques, researchers can develop advanced setups to investigate complex phenomena within the EDL. By placing a nanopore in an electrode and monitoring ion transport and capacitance at the single-molecule level, researchers can gain insights into ion mobility, charge screening, and molecular interactions within the EDL. This includes the development of multi-channel nanopore systems for high-throughput analysis, as well as combining nanopore studies with other analytical techniques, such as mass spectrometry or spectroscopy, for comprehensive characterizations of ion and molecule dynamics.

Surface charge and reactivity: Probing the correlation between the surface charge of electrodes and the behavior of ionic liquids within the EDL is essential for optimizing electrode-ionic liquid interfaces. Single-molecule techniques can be employed to examine how the surface charge of electrodes influences ion distribution, double-layer capacitance, and the reactivity of ionic liquids. This knowledge is crucial for various applications, including energy storage, conversion, and electrocatalysis.

In summary, the continuous development of single-molecule technologies and ionic liquids provides a broad prospect for scientific research and engineering applications. In this review, we summarize the recent progress in employing ionic liquids in single-molecule junctions, a forefront and rapidly evolving field of research. We illustrate the modulation mechanisms employed by ionic liquids in these junctions, highlighting their roles as gates, electrochemical controllers, and interfaces between molecules and electrodes. We thoroughly examine the diverse applications of single-molecule junctions involving ionic liquids, encompassing the creation of functional devices and the investigation of chemical reaction mechanism. At last, we propose the future research topics about the combination of ionic liquids and single-molecule junctions, which is expected to not only broaden our understanding of materials and devices at the atomic level, but also drive technological breakthroughs in fields like nanotechnology, energy, biotechnology, and quantum research.

CRediT authorship contribution statement

Li Zhou: Writing − original draft, Investigation, Formal analysis, Data curation, Conceptualization. **Miao Zhang:** Writing − original draft, Formal analysis, Conceptualization. **Yani Huo:** Writing − original draft. **Liping Bai:** Writing − review & editing. **Suhang He:** Writing − review & editing. **Jinying Wang:** Writing − review & editing, Project administration, Formal analysis, Conceptualization. **Chuancheng Jia:** Writing − review & editing, Project administration, Funding acquisition, Conceptualization. **Xuefeng Guo:** Writing − review & editing, Supervision, Project administration, Funding acquisition.

Conflict of interest

The authors declare that they have no known competing financial interests or personal relationships that could have appeared to influence the work reported in this paper.

Acknowledgments

References

[1] H. Chen, C. Jia, X. Zhu, C. Yang, X. Guo, J.F. Stoddart, Nat. Rev. Mater. 8 (2022) 165−185.

[2] H. Chen, W. Zhang, M. Li, G. He, X. Guo, Chem. Rev. 120 (2020) 2879−2949.

[3] P. Li, Y. Chen, B. Wang, M. Li, D. Xiang, C. Jia, X. Guo, Opto-Electron Adv. 5 (2022) 210094.

[4] T.A. Su, M. Neupane, M.L. Steigerwald, L. Venkataraman, C. Nuckolls, Nat. Rev. Mater. 1 (2016) 16002.

[5] H. Song, M.A. Reed, T. Lee, Adv. Mater. 23 (2011) 1583−1608.

[6] D. Xiang, X. Wang, C. Jia, T. Lee, X. Guo, Chem. Rev. 116 (2016) 4318−4440.

[7] S. Chen, D. Su, C. Jia, Y. Li, X. Li, X. Guo, D.A. Leigh, L. Zhang, Chem 8 (2022) 243−252.

[8] Y. Tan, J. Li, S. Li, H. Yang, T. Chi, S.B. Shiring, K. Liu, B.M. Savoie, B.W. Boudouris, C.M. Schroeder, Nano Lett. 23 (2023) 5951−5958.

[9] C. Jia, J. Wang, C. Yao, Y. Cao, Y. Zhong, Z. Liu, Z. Liu, X. Guo, Angew. Chem. Int. Ed. 52 (2013) 8666−8670.

[10] C. Jia, A. Migliore, N. Xin, S. Huang, J. Wang, Q. Yang, S. Wang, H. Chen, D. Wang, B. Feng, Z. Liu, G. Zhang, D.-H. Qu, H. Tian, M.A. Ratner, H.Q. Xu, A. Nitzan, X. Guo, Science 352 (2016) 1443−1445.

[11] X. Yin, Y. Zang, L. Zhu, J.Z. Low, Z.-F. Liu, J. Cui, J.B. Neaton, L. Venkataraman, L.M. Campos, Sci. Adv. 3 (2017) eaao2615.

[12] Y. Li, M. Buerkle, G. Li, A. Rostamian, H. Wang, Z. Wang, D.R. Bowler, T. Miyazaki, L. Xiang, Y. Asai, G. Zhou, N. Tao, Nat. Mater. 18 (2019) 357−363.

[13] S. Tao, Q. Zhang, A. Vezzoli, C. Zhao, C. Zhao, S.J. Higgins, A. Smogunov, Y.J. Dappe, R.J. Nichols, L. Yang, Phys. Chem. Chem. Phys. 24 (2022) 6836−6844.

[14] H. Song, Y. Kim, Y.H. Jang, H. Jeong, M.A. Reed, T. Lee, Nature 462 (2009) 1039−1043.

[15] H. Liu, L. Chen, H. Zhang, Z. Yang, J. Ye, P. Zhou, C. Fang, W. Xu, J. Shi, J. Liu, Y. Yang, W. Hong, Nat. Mater. 22 (2023) 1007−1012.

[16] B.F. Zeng, G. Wang, Q.Z. Qian, Z.X. Chen, X.G. Zhang, Z.X. Lu, S.Q. Zhao, A.N. Feng, J. Shi, Y. Yang, W. Hong, Small 16 (2020) 2004720.

[17] H. Chen, V. Brasiliense, J. Mo, L. Zhang, Y. Jiao, Z. Chen, L.O. Jones, G. He, Q.-H. Guo, X.-Y. Chen, B. Song, G.C. Schatz, J.F. Stoddart, J. Am. Chem. Soc. 143 (2021) 2886−2895.

[18] H. Liu, H. Zhang, Y. Zhao, J. Liu, W. Hong, Trends Chem 5 (2023) 367−379.

[19] O. Adak, E. Rosenthal, J. Meisner, E.F. Andrade, A.N. Pasupathy, C. Nuckolls, M.S. Hybertsen, L. Venkataraman, Nano Lett. 15 (2015) 4143−4149.

[20] M.-W. Gu, H.H. Peng, I.W.P. Chen, C.-H. Chen, Nat. Mater. 20 (2021) 658−664.

[21] N. Xin, J. Guan, C. Zhou, X. Chen, C. Gu, Y. Li, M.A. Ratner, A. Nitzan, J.F. Stoddart, X. Guo, Nat. Rev. Phys. 1 (2019) 211−230.

[22] K.B. Oldham, J. Electroanal. Chem. 613 (2008) 131−138.

[23] K. Ma, R. Jarosova, G.M. Swain, G.J. Blanchard, Langmuir 32 (2016) 9507−9512.

[24] M. Armand, F. Endres, D.R. Macfarlane, H. Ohno, B. Scrosati, Nat. Mater. 8 (2009) 621−629.

[25] T. Torimoto, T. Tsuda, K.-I. Okazaki, S. Kuwabata, Adv. Mater. 22 (2010) 1196−1221.

[26] L. Chen, C. Zhao, X. Duan, J. Zhou, M. Liu, CCS Chem. 4 (2022) 1386−1396.

[27] M. Zhang, Z. Wu, H. Jia, P. Li, L. Yang, J. Hao, J. Wang, E. Zhang, L. Meng, Z. Yan, Y. Liu, P. Du, X. Kong, S. Xiao, C. Jia, X. Guo, Sci. Adv. 9 (2023) eadg4346.

[28] S.R. Catarelli, S.J. Higgins, W. Schwarzacher, B.-W. Mao, J.-W. Yan, R.J. Nichols, Langmuir 30 (2014) 14329−14336.

[29] Z. Li, H. Li, S. Chen, T. Froehlich, C. Yi, C. Schönenberger, M. Calame, S. Decurtins, S.-X. Liu, E. Borguet, J. Am. Chem. Soc. 136 (2014) 8867−8870.

[30] Y. Li, W. Xu, Y.L. Zou, J. Li, T. Gao, R. Huang, L. Chen, Z. Xiao, J. Shi, Y. Yang, W. Hong, Adv. Funct. Mater. 33 (2023) 2302985.

[31] T. Albrecht, K. Moth-Poulsen, J.B. Christensen, J. Hjelm, T. Bjørnholm, J. Ulstrup, J. Am. Chem. Soc. 128 (2006) 6574−6575.

[32] Y. Zhao, W. Liu, J. Zhao, Y. Wang, J. Zheng, J. Liu, W. Hong, Z.-Q. Tian, Int. J. Extrem. Manuf. 4 (2022) 022003.

[33] H. Suga, H. Suzuki, K. Otsu, T. Abe, Y. Umeta, K. Tsukagoshi, T. Sumiya, H. Shima, H. Akinaga, Y. Naitoh, ACS Appl. Nano Mater. 3 (2020) 4077−4083.

[34] M. Tsutsui, M. Taniguchi, Sensors 12 (2012) 7259−7298.

[35] C. Yang, A. Qin, B.Z. Tang, X. Guo, J. Chem. Phys. 152 (2020) 120920.

[36] O.S. Lumbroso, L. Simine, A. Nitzan, D. Segal, O. Tal, Nature 562 (2018) 240−244.

[37] M.H. Garner, H. Li, Y. Chen, T.A. Su, Z. Shangguan, D.W. Paley, T. Liu, F. Ng, H. Li, S. Xiao, C. Nuckolls, L. Venkataraman, G.C. Solomon, Nature 558 (2018) 415−419.

[38] L. Venkataraman, J.E. Klare, C. Nuckolls, M.S. Hybertsen, M.L. Steigerwald, Nature 442 (2006) 904−907.

[39] P. Li, S. Hou, B. Alharbi, Q. Wu, Y. Chen, L. Zhou, T. Gao, R. Li, L. Yang, X. Chang, G. Dong, X. Liu, S. Decurtins, S.-X. Liu, W. Hong, C.J. Lambert, C. Jia, X. Guo, J. Am. Chem. Soc. 144 (2022) 15689−15697.

[40] R.C. Chiechi, E.A. Weiss, M.D. Dickey, G.M. Whitesides, Angew. Chem. Int. Ed. 47 (2008) 142−144.

[41] Y. Han, C. Nickle, Z. Zhang, H.P.a.G. Astier, T.J. Duffin, D. Qi, Z. Wang, E. Del Barco, D. Thompson, C.A. Nijhuis, Nat. Mater. 19 (2020) 843−848.

[42] R. Hoffmann-Vogel, Appl. Phys. Rev. 4 (2017) 031302.

[43] X. Guo, J.P. Small, J.E. Klare, Y. Wang, M.S. Purewal, I.W. Tam, B.H. Hong, R. Caldwell, L. Huang, S. O'brien, J. Yan, R. Breslow, S.J. Wind, J. Hone, P. Kim, C. Nuckolls, Science 311 (2006) 356−359.

[44] Y. Cao, S. Dong, S. Liu, L. He, L. Gan, X. Yu, M.L. Steigerwald, X. Wu, Z. Liu, X. Guo, Angew. Chem. Int. Ed. 51 (2012) 12228−12232.

[45] H. Park, A.K.L. Lim, A.P. Alivisatos, J. Park, P.L. Mceuen, Appl. Phys. Lett. 75 (1999) 301−303.

[46] D.R. Strachan, D.E. Smith, D.E. Johnston, T.H. Park, M.J. Therien, D.A. Bonnell, A.T. Johnson, Appl. Phys. Lett. 86 (2005) 043109.

[47] P.G. Collins, M. Hersam, M. Arnold, R. Martel, P. Avouris, Phys. Rev. Lett. 86 (2001) 3128−3131.

[48] F. Prins, A. Barreiro, J.W. Ruitenberg, J.S. Seldenthuis, N. Aliaga-Alcalde, L.M.K. Vandersypen, H.S.J. Van Der Zant, Nano Lett. 11 (2011) 4607−4611.

[49] S. V. Aradhya, M. Frei, M. S. Hybertsen, L. Venkataraman, 11 (2012) 872−876.

[50] W. Haiss, R.J. Nichols, H. Van Zalinge, S.J. Higgins, D. Bethell, D.J. Schiffrin, Phys. Chem. Chem. Phys. 6 (2004) 4330−4337.

[51] B. Xu, N. Tao, Science 301 (2003) 1221−1223.

[52] M.A. Reed, C. Zhou, C.J. Muller, T.P. Burgin, J.M. Tour, Science 278 (1997) 252−254.

[53] J. Bai, A. Daaoub, S. Sangtarash, X. Li, Y. Tang, Q. Zou, H. Sadeghi, S. Liu, X. Huang, Z. Tan, J. Liu, Y. Yang, J. Shi, G. Mészáros, W. Chen, C. Lambert, W. Hong, Nat. Mater. 18 (2019) 364−369.

[54] Y.S. Park, A.C. Whalley, M. Kamenetska, M.L. Steigerwald, M.S. Hybertsen, C. Nuckolls, L. Venkataraman, J. Am. Chem. Soc. 129 (2007) 15768−15769.

[55] S.a.G. Vrouwe, E. Van Der Giessen, S.J. Van Der Molen, D. Dulic, M.L. Trouwborst, B.J. Van Wees, Phys. Rev. B 71 (2005) 035313.

[56] J. Moreland, J.W. Ekin, Appl. Phys. Lett. 47 (1985) 175−177.

[57] X. Li, Q. Wu, J. Bai, S. Hou, W. Jiang, C. Tang, H. Song, X. Huang, J. Zheng, Y. Yang, J. Liu, Y. Hu, J. Shi, Z. Liu, C.J. Lambert, D. Zhang, W. Hong, Angew. Chem. Int. Ed. 59 (2020) 3280−3286.

[58] P. Makk, D. Tomaszewski, J. Martinek, Z. Balogh, S. Csonka, M. Wawrzyniak, M. Frei, L. Venkataraman, A. Halbritter, ACS Nano 6 (2012) 3411−3423.

[59] N. Xin, X. Kong, Y.P. Zhang, C. Jia, L. Liu, Y. Gong, W. Zhang, S. Wang, G. Zhang, H.L. Zhang, H. Guo, X. Guo, Adv. Electron. Mater. 6 (2020) 1901237.

[60] M.M. Elmahdy, T. Fahmy, K.A. Aldhafeeri, E.O. Ibnouf, Y. Riadi, Mater. Chem. Phys. 264 (2021) 124369.

[61] M. Shamsipur, A.a.M. Beigi, M. Teymouri, S.M. Pourmortazavi, M. Irandoust, J. Mol. Liq. 157 (2010) 43−50.

[62] Z. Li, Z. Fan, Y. Lian, Z. Chen, New J. Chem. 45 (2021) 17163−17175.

[63] J. Sanes, F.-J. Carrión, M.-D. Bermúdez, Appl. Surf. Sci. 255 (2009) 4859−4862.

[64] I.-N. Yoon, S. Yoo, S.-J. Park, J. Won, Chem. Eng. J. 172 (2011) 237−242.

[65] D. Fang, C. Zhou, G. Liu, G. Luo, P. Gong, Q. Yang, Y. Niu, G. Li, Polymer 148 (2018) 68−78.

[66] K.A. Motghare, D.Z. Shende, K.L. Wasewar, J. Chem. Technol. Biotechnol. 97 (2021) 873−884.

[67] J.T. Ye, S. Inoue, K. Kobayashi, Y. Kasahara, H.T. Yuan, H. Shimotani, Y. Iwasa, Nat. Mater. 9 (2009) 125−128.

[68] F. Wang, P. Stepanov, M. Gray, C.N. Lau, M.E. Itkis, R.C. Haddon, Nano Lett. 15 (2015) 5284−5288.

[69] Y. Pei, Y. Zhang, J. Ma, M. Fan, S. Zhang, J. Wang, Mater. Today Nano. 17 (2022) 100159.

[70] T. Stettner, A. Balducci, Energy Storage Mater. 40 (2021) 402−414.

[71] M.V. Fedorov, A.A. Kornyshev, Chem. Rev. 114 (2014) 2978−3036.

[72] S. Zhou, K.S. Panse, M.H. Motevaselian, N.R. Aluru, Y. Zhang, ACS Nano 14 (2020) 17515−17523.

[73] N. Xin, X. Li, C. Jia, Y. Gong, M. Li, S. Wang, G. Zhang, J. Yang, X. Guo, Angew. Chem. Int. Ed. 57 (2018) 14026−14031.

[74] M.M. Islam, M.T. Alam, T. Ohsaka, J. Phys. Chem. C 112 (2008) 16568−16574.

[75] W. Jin, X. Liu, Y. Han, S. Li, T. Yan, Phys. Chem. Chem. Phys. 17 (2015) 2628−2633.

[76] C.W. Lopes, P.H. Finger, M.L. Mignoni, D.J. Emmerich, F.M.T. Mendes, S. Amorim, S.B.C. Pergher, Microporous Mesoporous Mater. 213 (2015) 78−84.

[77] Y. Kim, Y. Matsuzawa, S. Ozaki, K. Park, C. Kim, M. Endo, H. Yoshida, G. Masuda, T. Sato, M. Dresselhaus, J. Electrochem. Soc. 152 (2005) 710.

[78] J. Zhou, Y. Zheng, S. Dong, Z. He, B. Liu, Y. Zhang, Curr. Appl. Phys. 52 (2023) 45−56.

[79] M. Hayyan, F.S. Mjalli, M.A. Hashim, I.M. Alnashef, T.X. Mei, J. Ind. Eng. Chem. 19 (2013) 106−112.

[80] S.P. Ong, O. Andreussi, Y. Wu, N. Marzari, G. Ceder, Chem. Mater. 23 (2011) 2979−2986.

[81] K. Liu, Y.-X. Zhou, H.-B. Han, S.-S. Zhou, W.-F. Feng, J. Nie, H. Li, X.-J. Huang, M. Armand, Z.-B. Zhou, Electrochim. Acta 55 (2010) 7145−7151.

[82] T. Belhocine, S.A. Forsyth, H.Q.N. Gunaratne, M. Nieuwenhuyzen, A.V. Puga, K.R. Seddon, G. Srinivasan, K. Whiston, Green Chem. 13 (2011) 59−63.

[83] D.R. Macfarlane, P. Meakin, J. Sun, N. Amini, M. Forsyth, J. Phys. Chem. B 103 (1999) 4164−4170.

[84] P. Bonhôte, A.-P. Dias, N. Papageorgiou, K. Kalyanasundaram, M. Grätzel, Inorg. Chem. 35 (1996) 1168−1178.

[85] P. Hapiot, C. Lagrost, Chem. Rev. 108 (2008) 2238−2264.

[86] G.B. Appetecchi, M. Montanino, D. Zane, M. Carewska, F. Alessandrini, S. Passerini, Electrochim. Acta 54 (2009) 1325−1332.

[87] M. Montanino, M. Carewska, F. Alessandrini, S. Passerini, G.B. Appetecchi, Electrochim. Acta 57 (2011) 153−159.

[88] P.a.Z. Suarez, V.M. Selbach, J.E.L. Dullius, S. Einloft, C.M.S. Piatnicki, D.S. Azambuja, R.F. De Souza, J. Dupont, Electrochim. Acta 42 (1997) 2533−2535.

[89] Z. Xue, L. Qin, J. Jiang, T. Mu, G. Gao, Phys. Chem. Chem. Phys. 20 (2018) 8382−8402.

[90] S.S. Moganty, R.E. Baltus, D. Roy, Chem. Phys. Lett. 483 (2009) 90−94.

[91] B.D. Fitchett, T.N. Knepp, J.C. Conboy, J. Electrochem. Soc. 151 (2004) 219.

[92] A. O'mahony, D. Silvester, L. Aldous, C. Hardacre, R. Compton, J. Chem. Eng. Data 53 (2008) 2884−2891.

[93] H. Fu, X. Zhu, P. Li, M. Li, L. Yang, C. Jia, X. Guo, J. Mater. Chem. C 10 (2022) 2375−2389.

[94] Y. Fei, Z. Chen, J. Zhang, M. Yu, J. Kong, Z. Wu, J. Cao, J. Zhang, J. Mol. Liq. 342 (2021) 117553.

[95] X. Yu, Z. Xia, T. Zhao, X. Yuan, L. Ren, Macromolecules 54 (2021) 4227−4235.

[96] H. Helmholtz, Ann. Phys. 165 (1853) 211−233.

[97] M. Gouy, J. phys. theor. appl. 9 (1910) 457−468.

[98] D.L. Chapman, The London, Edinburgh, and Dublin Philosophical Magazine and, J. Sci. 25 (1913) 475−481.

[99] O. Stern, Zeitschrift für Elektrochemie und angewandte physikalische Chemie 30 (1924) 508−516.

[100] T. Fujimoto, K. Awaga, Phys. Chem. Chem. Phys. 15 (2013).

[101] D.C. Grahame, Chem. Rev. 41 (1947) 441−501.

[102] X. Wang, M. Salari, D.-E. Jiang, J. Chapman Varela, B. Anasori, D. Wesolowski, S. Dai, M. Grinstaff, Y. Gogotsi, Nat. Rev. Mater. 5 (2020) 787−808.

[103] M.G. Del Pópolo, G.A. Voth, J. Phys. Chem. B 108 (2004) 1744−1752.

[104] A.L. Kiratidis, S.J. Miklavcic, J. Chem. Phys. 150 (2019) 184502.

[105] A.A. Kornyshev, J. Phys. Chem. B 111 (2007) 5545−5557.

[106] D.-E. Jiang, D. Meng, J. Wu, Chem. Phys. Lett. 504 (2011) 153−158.

[107] V. Ivaništšev, S. O'connor, M.V. Fedorov, Electrochem. Commun. 48 (2014) 61−64.

[108] M.Z. Bazant, B.D. Storey, A.A. Kornyshev, Phys. Rev. Lett. 106 (2011) 046102.

[109] M. Mezger, H. Schröder, H. Reichert, S. Schramm, J.S. Okasinski, S. Schöder, V. Honkimäki, M. Deutsch, B.M. Ocko, J. Ralston, M. Rohwerder, M. Stratmann, H. Dosch, Science 322 (2008) 424−428.

[110] R. Hayes, N. Borisenko, M.K. Tam, P.C. Howlett, F. Endres, R. Atkin, J. Phys. Chem. C 115 (2011) 6855−6863.

[111] J.M. Black, D. Walters, A. Labuda, G. Feng, P.C. Hillesheim, S. Dai, P.T. Cummings, S.V. Kalinin, R. Proksch, N. Balke, Nano Lett. 13 (2013) 5954−5960.

[112] B. Capozzi, J. Xia, O. Adak, E.J. Dell, Z.-F. Liu, J.C. Taylor, J.B. Neaton, L.M. Campos, L. Venkataraman, Nat. Nanotechnol. 10 (2015) 522−527.

[113] B. Capozzi, Q. Chen, P. Darancet, M. Kotiuga, M. Buzzeo, J.B. Neaton, C. Nuckolls, L. Venkataraman, Nano Lett. 14 (2014) 1400−1404.

[114] R.J. Nichols, S.J. Higgins, Acc. Chem. Res. 49 (2016) 2640−2648.

[115] P. Li, C. Jia, X. Guo, Chem. Rec. 21 (2021) 1284−1299.

[116] P. Li, L. Zhou, C. Zhao, H. Ju, Q. Gao, W. Si, L. Cheng, J. Hao, M. Li, Y. Chen, C. Jia, X. Guo, Rep. Prog. Phys. 85 (2022) 086401.

[117] C. Jia, X. Guo, Chem. Soc. Rev. 42 (2013) 5642−5660.

[118] X. Xie, P. Li, Y. Xu, L. Zhou, Y. Yan, L. Xie, C. Jia, X. Guo, ACS Nano 16 (2022) 3476−3505.

[119] K. Moth-Poulsen, T. Bjørnholm, Nat. Nanotechnol. 4 (2009) 551−556.

[120] J. Bai, X. Li, Z. Zhu, Y. Zheng, W. Hong, Adv. Mater. 33 (2021) 2005883.

[121] Y. Han, C.A. Nijhuis, Chem. Asian J. 15 (2020) 3752−3770.

[122] N.J. Kay, S.J. Higgins, J.O. Jeppesen, E. Leary, J. Lycoops, J. Ulstrup, R.J. Nichols, J. Am. Chem. Soc. 134 (2012) 16817−16826.

[123] W. Haiss, T. Albrecht, H. Van Zalinge, S.J. Higgins, D. Bethell, H. Höbenreich, D.J. Schiffrin, R.J. Nichols, A.M. Kuznetsov, J. Zhang, Q. Chi, J. Ulstrup, J. Phys. Chem. B 111 (2007) 6703−6712.

[124] H.M. Osorio, S. Catarelli, P. Cea, J.B.G. Gluyas, F. Hartl, S.J. Higgins, E. Leary, P.J. Low, S. Martín, R.J. Nichols, J. Tory, J. Ulstrup, A. Vezzoli, D.C. Milan, Q. Zeng, J. Am. Chem. Soc. 137 (2015) 14319−14328.

[125] Y. Li, H. Wang, Z. Wang, Y. Qiao, J. Ulstrup, H.-Y. Chen, G. Zhou, N. Tao, Proc. Natl. Acad. Sci. U.S.A. 116 (2019) 3407−3412.

[126] Z. Yu, Y.X. Xu, J.Q. Su, P.M. Radjenovic, Y.H. Wang, J.F. Zheng, B. Teng, Y. Shao, X.S. Zhou, J.F. Li, Angew. Chem. Int. Ed. 60 (2021) 15452−15458.

[127] Z. Yu, J.-Q. Li, Y.-H. Wang, J.-Q. Su, J.-Y. Fu, J.-W. Zou, J.-F. Zheng, Y. Shao, X.-S. Zhou, Anal. Chem. 94 (2022) 1823−1830.

[128] J. Li, S. Pudar, H. Yu, S. Li, J.S. Moore, J. Rodríguez-López, N.E. Jackson, C.M. Schroeder, J. Phys. Chem. C 125 (2021) 21862−21872.

[129] B. Huang, X. Liu, Y. Yuan, Z.-W. Hong, J.-F. Zheng, L.-Q. Pei, Y. Shao, J.-F. Li, X.-S. Zhou, J.-Z. Chen, S. Jin, B.-W. Mao, J. Am. Chem. Soc. 140 (2018) 17685−17690.

[130] C. Jia, M. Famili, M. Carlotti, Y. Liu, P. Wang, I.M. Grace, Z. Feng, Y. Wang, Z. Zhao, M. Ding, X. Xu, C. Wang, S.-J. Lee, Y. Huang, R.C. Chiechi, C.J. Lambert, X. Duan, Sci. Adv. 4 (2018) eaat8237.

[131] M. Famili, C. Jia, X. Liu, P. Wang, I.M. Grace, J. Guo, Y. Liu, Z. Feng, Y. Wang, Z. Zhao, S. Decurtins, R. Häner, Y. Huang, S.-X. Liu, C.J. Lambert, X. Duan, Chem 5 (2019) 474−484.

[132] H. Fu, C. Zhao, J. Cheng, S. Zhou, P. Peng, J. Hao, Z. Liu, X. Gao, C. Jia, X. Guo, J. Mater. Chem. C 10 (2022) 7803−7809.

[133] M. Li, H. Fu, B. Wang, J. Cheng, W. Hu, B. Yin, P. Peng, S. Zhou, X. Gao, C. Jia, X. Guo, J. Am. Chem. Soc. 144 (2022) 20797−20803.

[134] Z. Yan, X. Li, Y. Li, C. Jia, N. Xin, L. Peihui, L. Meng, M. Zhang, L. Chen, J. Yang, R. Wang, X. Guo, Sci. Adv. 8 (2022) eabm3541.

[135] N. Xin, C. Hu, H. Al Sabea, M. Zhang, C. Zhou, L. Meng, C. Jia, Y. Gong, Y. Li, G. Ke, X. He, P. Selvanathan, L. Norel, M.A. Ratner, Z. Liu, S. Xiao, S. Rigaut, H. Guo, X. Guo, J. Am. Chem. Soc. 143 (2021) 20811−20817.

[136] L. Zhang, C. Yang, C. Lu, X. Li, Y. Guo, J. Zhang, J. Lin, Z. Li, C. Jia, J. Yang, K.N. Houk, F. Mo, X. Guo, Nat. Commun. 13 (2022) 4552.

[137] S. Naghibi, S. Sangtarash, V.J. Kumar, J.Z. Wu, M.M. Judd, X. Qiao, E. Gorenskaia, S.J. Higgins, N. Cox, R.J. Nichols, H. Sadeghi, P.J. Low, A. Vezzoli, Angew. Chem. Int. Ed. 61 (2022) e202116985.

[138] Y. Li, M. Baghernejad, A.-G. Qusiy, D. Zsolt Manrique, G. Zhang, J. Hamill, Y. Fu, P. Broekmann, W. Hong, T. Wandlowski, D. Zhang, C. Lambert, Angew. Chem. Int. Ed. 54 (2015) 13586−13589.